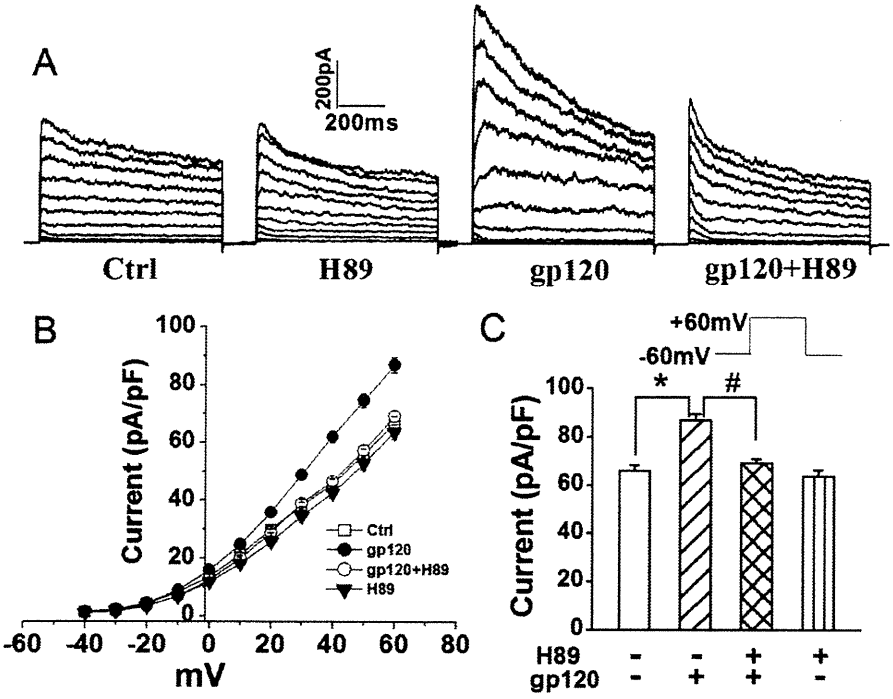

Fig. 5. Blockade of gp120-induced enhancement of outward K^+ currents by H89, a specific inhibitor for PKA. **A**: Representative current traces recorded from a control cell (Ctrl) and cells treated respectively with H89 alone, gp120 alone, and gp120+H89. The voltage protocol used to generate outward K^+ current was the same as the one shown in Fig. 1. **B**: I–V relationship illustrating the outward K^+ current densities as a function of voltage from the current traces shown in A. **C**: Summarized bar graphs showing average outward K^+ current densities measured at a voltage step +60 mV from microglia treated with H89 alone, gp120 alone, and gp120+H89. Note a significant blockade of gp120 enhancement of outward K^+ currents recorded in microglia. * $P < 0.05$ vs. ctrl, # $P < 0.05$ vs. gp120.

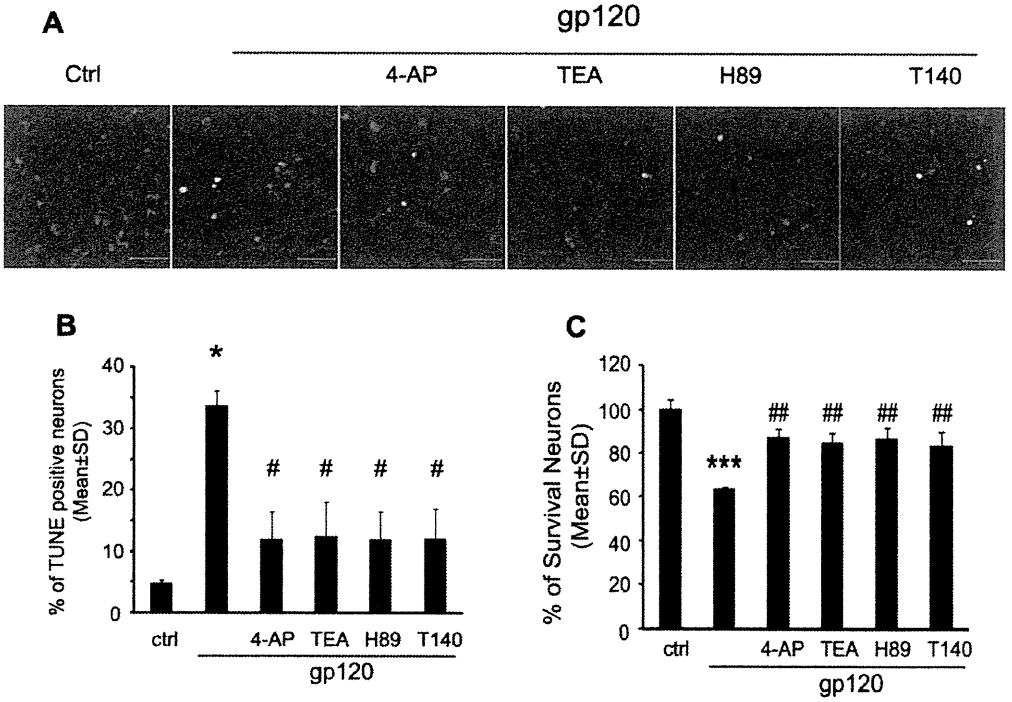

Fig. 6. Gp120-activated microglia produced cytotoxicity on neurons. Panel A: apoptotic neurons were visualized by TUNEL staining at ×400 original magnification (scale bar 50 μm). Panel B: Neuronal apoptosis was analyzed by combined TUNEL/DAPI staining and percentage of apoptotic neurons was determined by TUNEL-positive cells to normalize the total number of DAPI-positive cells. Compared with control group, an increasing percentage of apoptotic neurons were notably observed in gp120 treated group (Control vs. gp120, 7.7% vs. 33.77%). The apoptosis induced by gp120-stimulated microglia were attenuated by 4-AP, TEA, H89, and T140. Panel C: Neuronal viability was assessed by MTT assay. 4-AP, TEA, H89, and T140 significantly attenuated the neurotoxic activity of gp120-stimulated microglia. Values are expressed as mean ± SD of triplicate cultures. The results are representative of three independent experiments performed in triplicate determinations. *$P < 0.05$, ***$P < 0.001$ vs. Ctrl, # $P < 0.05$, ## $P < 0.01$ vs. gp120.

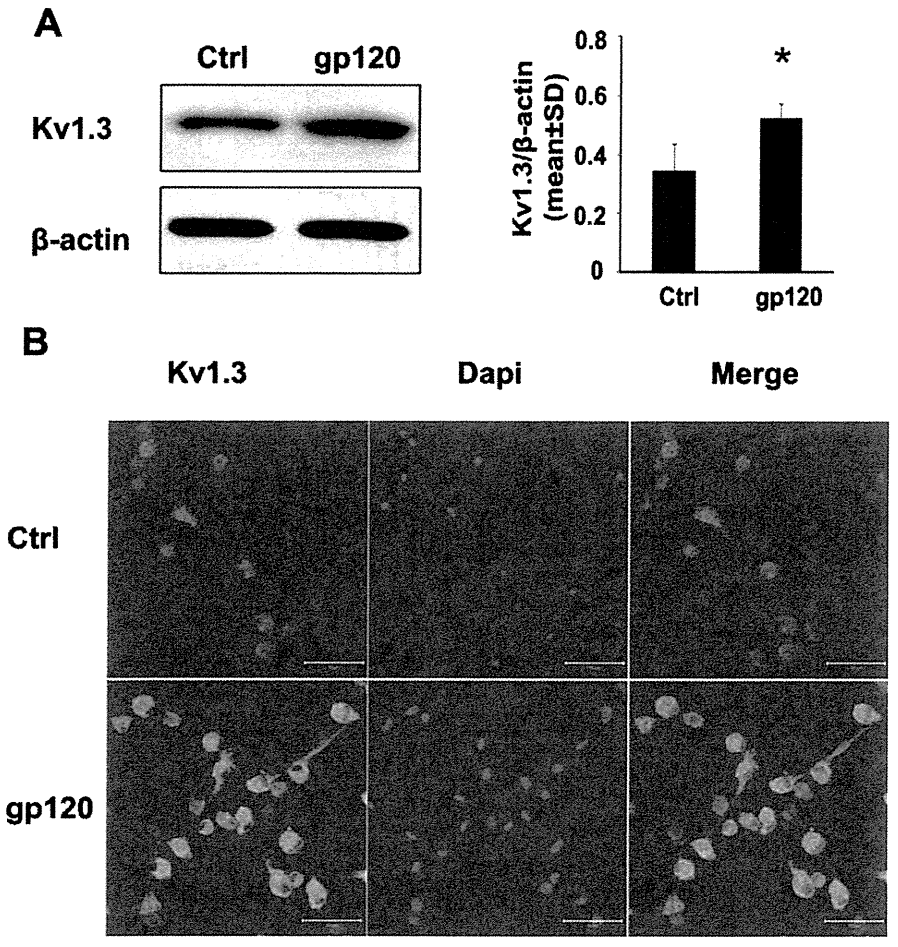

Fig. 7. gp120 enhanced expression levels of $K_v1.3$ in cultured microglia. Rat microglia (2×10^6 cells/well in 6 well plates or 0.5×10^6 cells/well in 24 well plates) were treated with or without gp120 (500 pM) for 24 h. The expression levels of $K_v1.3$ channel proteins were examined by Western blot and immunocytochemistry. Panel A: the representative scans showed Western blots for $K_v1.3$, and internal control β-actin (left). Each band density was normalized to its internal control and represents in bar graphs (right). Significant differences were detected in gp120 (1.5-fold increase) compared with nontreated microglia. $^*P < 0.05$ in comparison to control group were analyzed using Student's *t*-test. Panel B: Microglia were immunostained for expression of $K_v1.3$ (green). Images were visualized by fluorescent confocal microscopy at ×400 original magnification (scale bar 50 μm).

a significant neuronal apoptosis when co-cultured with neurons (data not shown).

Effects of gp120 on Microglia K_v Channel Expression

The voltage dependence of activation and inactivation of the outward K^+ current recorded in rat microglia, plus its blockade by 4-AP and TEA, suggest a possible identity of $K_v1.3$ current, which is in agreement with the up-regulated expression levels of $K_v1.3$ mRNA observed by other investigators (Eder, 1998; Norenberg et al., 1994; Schilling et al., 2000). To assess whether gp120 alters $K_v1.3$ protein expression, we examined the expression levels of $K_v1.3$ protein in microglia (2×10^6 cells/well, in six well plates) treated with or without gp120 for 24 h by western blot and immunocytochemistry. Our results showed that gp120 enhanced both the expression levels of $K_v1.3$ channel protein and immunofluorescent density of $K_v1.3$ staining in cultured microglia (see Fig. 7). The increase of $K_v1.3$ channel expression following gp120 treatment may underlie gp120-associated enhancement of outward K^+ current recorded in rat microglia.

Specific $K_v1.3$ Antagonist Blocks gp120-Induced Increase of Outward K^+ Current and Neuronal Apoptosis

After demonstration of gp120 enhancement of $K_v1.3$ expression, we further verified if the newly formed channels were functionally active and involved in gp120-associated increase of outward K^+ current and neuronal apoptosis using a specific $K_v1.3$ blocker margatoxin, MgTx, (Knaus et al., 1995). In another group of experiments, incubation of microglia with gp120 produced a signifi-

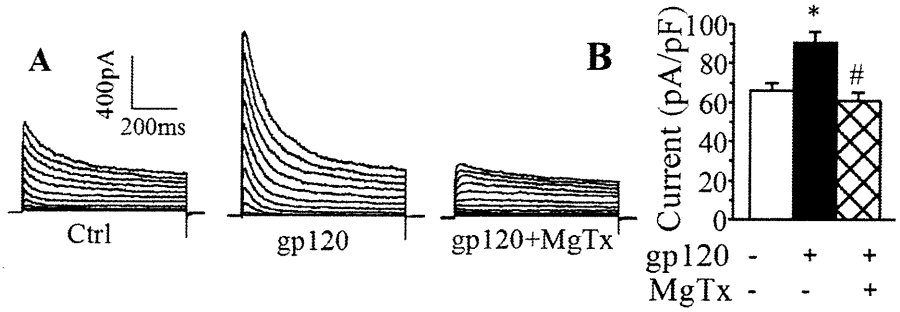

Fig. 8. Blockade of gp120 enhancement of outward K^+ current by MgTx, a specific $K_v1.3$ blocker. **A**: An example showing blockade of gp120-induced enhancement of outward K^+ current in rat microglia by MgTx. **B**: A summary bar graph illustrating MgTx significantly blocked gp120-induced enhancement of microglia outward K^+ current. Instantaneous outward K^+ current generated by a voltage step from −60 to +60 mV were measured and current densities were calculated. *, $P <$ 0.01 gp120-MgTx- vs. gp120+MgTx-; #, $P < 0.01$ gp120+MgTx- vs. gp120+MgTx+.

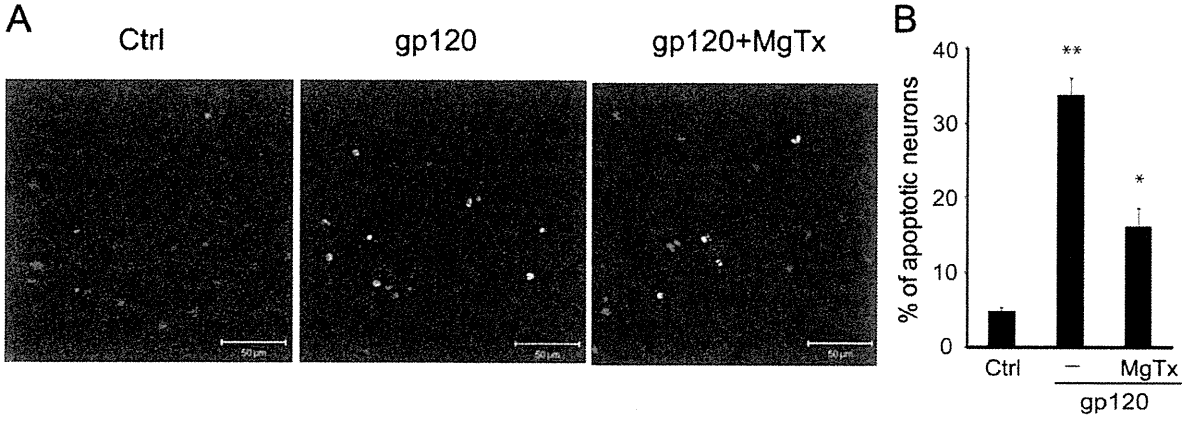

Fig. 9. Neurotoxic activity induced by gp120-stimulated microglia was blocked by MgTx in a microglia-neuronal co-culture system. **A**: Apoptotic neurons were assayed by TUNEL staining and visualized (green) via confocal microscopy at ×400 original magnifications. Scale bar equals 50 μM. **B**: Quantification of apoptotic neurons was made by enumeration of TUNEL-positive cells and expressed as percentage of total number of DAPI-positive cells counted. Note that gp120-stimulated microglia produced a significant increase of apoptotic neurons and the blockade of microglia $K_v1.3$ channel by MgTx significantly reduced microglia-induced neuronal apoptosis.

cant ($P < 0.01$) enhancement of outward K^+ current with an average current density of 90.4 ± 5.7 pA/pF (Fig. 8; $n = 12$) when compared with the current density (65.7 ± 4.3 pA/pF, $n = 10$) recorded in control (without gp120 treatment) microglia. Addition of MgTx (100 nM) to the bath solution abolished gp120-induced increase of outward K^+ current with an average of instantaneous current density of 60.5 ± 4.5 pA/pF (Fig. 8; $n = 8$). In comparison with the current density recorded in microglia treated with gp120, the difference was statistically significant ($P < 0.01$). The involvement of $K_v1.3$ in gp120-innduced neuronal injury was demonstrated by the results showing a significant attenuation of gp120-induced neuronal apoptosis by pretreatment of microglia with MgTx in microglia-neuronal co-culture system as shown in Fig. 9. These results indicate that the newly formed $K_v1.3$ channels were functional and involved in gp120-associated enhancement of outward K^+ current in rat microglia.

DISCUSSION

As the targets for HIV-1 infection and the producers of neurotoxins, microglia play an important role in the pathogenesis of HAND and other neurodegenerative disorders. It is widely accepted that the infected and immune-activated microglia secrete a variety of bioactive substances including viral protein gp120, resulting in neuronal dysfunction and death (Garden, 2002; Glass and Wesselingh, 2001). The mechanisms underlying microglia-associated neuropathogenesis are not fully understood. In this study, we demonstrated that HIV-1 gp120 increased the levels of $K_v1.3$ expression and enhanced outward K^+ current in cultured rat microglia via CXCR4-PKA signaling pathways. The enhancement of outward K^+ current was associated with microglia neurotoxicity evident through experimental results showing the blockade of microglia $K_v1.3$ channels suppressed microglia-associated neurotoxicity *in vitro*.

In HIV-1-infected brain, gp120, shed from virions and/or secreted from HIV-1-infected microglia/macrophages, has the potential to diffuse and interact directly with surrounding and distant neural cells through activation of CXCR4 receptors(Bachis and Mocchetti, 2004; Hesselgesser et al., 1998; Meucci et al., 1998), or by stimulation of uninfected microglia to release neurotoxins which act indirectly on local and distant neural cells, or both. Transgenic mice expressing gp120 manifest a spectrum of neuronal and glial changes resembling abnormalities in brains of HIV-1-infected humans and the severity of damage correlated positively with brain levels of gp120 expression (Toggas et al., 1994). While the precise mechanisms on how gp120 stimulates microglia production of neurotoxins remains to be determined, the enhancement of outward K^+ current by gp120 through CXCR4 may represent one of such potential mechanisms, as microglia-associated neurotoxicity was blocked either by a CXCR4 antagonist or by K_v channel blockers.

Microglia express a defined pattern of K_v channels, which is distinct from other glial cells and neurons. This pattern undergoes defined changes with microglia activation. It is believed that microglia K_v channels, albeit in a lower density than their excitable counterparts, play an important role in the switch from one functional state to another (Farber and Kettenmann, 2005; Kotecha and Schlichter, 1999). Patch clamp studies of microglia in cell cultures and in tissue slices have demonstrated that outward rectifier $K_v1.3$ and $K_v1.5$ are dominant K_v channels (Eder, 1998; Kotecha and Schlichter, 1999; Newell and Schlichter, 2005; Pannasch et al., 2006; Schilling et al., 2000). Our results showed that elevated levels of $K_v1.3$ expression and enhanced outward K^+ currents were detected in gp120-stimulated microglia and that the neuronal apoptosis induced by gp120-stimulated microglia was blocked by K_v channel blockers. These results suggest that gp120-induced elevation of K_v channel expression and enhancement of outward K^+ current might trigger microglia-associated neurotoxicity. Whereas the functional roles of $K_v1.3$ in microglia remain to be determined, evidence from this study and others indicates that the newly formed $K_v1.3$ channels appear to be involved in microglia activation and subsequent production of neurotoxins (Eder, 1998, 2005; Fordyce et al., 2005; Kotecha and Schlichter, 1999).

Ion channels are the targets of many intracellular signaling pathways including protein phosphorylation. These processes can modify channel activity and alter cellular electrophysiological properties. Thus, protein phosphorylation is an important physiological regulator of K_v channel function. Amino acid sequences of $K_v1.3$ clones from mouse, rats and human are very similar, with >98% homology between human and rat clones (Chandy and Gutman, 1995). All $K_v1.3$ clones contain several potential PKA and PKC phosphorylation sites, with one strong PKA site at the COOH terminus (Kennelly and Krebs, 1991). Evidence that $K_v1.3$ channels can be regulated by PKA includes reports of enhancement of delayed rectifier K^+ currents in vascular smooth muscle cells (Aiello et al., 1995), squid giant axon (Perozo et al., 1989) and human T lymphocytes (Chung and Schlichter, 1997). Inhibition of serine/threonine protein phosphatases with okadaic acid increases $K_v1.3$ current and shifts the voltage dependence of activation and inactivation to more positive potentials. Inhibition of PKA by a specific PKA inhibitor decreases $K_v1.3$ current. These observations indicate that $K_v1.3$ activity can be regulated by serine/threonine phosphorylation. The results obtained in this study revealed that the gp120-induced enhancement of microglia outward K^+ current was blocked by a specific PKA inhibitor H89, suggesting that activation of CXCR4 by gp120 in microglia causes cAMP-dependent PKA activation, resulting in $K_v1.3$ phosphorylation and consequent enhancement of channel activity.

$K_v1.3$ is predominantly expressed in immunocytes including microglia, lymphocytes, and macrophages and is important for immunocyte-mediated immune and inflammatory responses (Beeton et al., 2006; Chandy et al., 2004). Mounting evidence suggests that immune and inflammatory responses mediated by the activated microglia, the predominant resident CNS cell type productively infected by HIV-1(Lipton and Gendelman, 1995), play a pivotal role in the pathogenesis of HAND (Dheen et al., 2007; Garden, 2002; Glass and Wesselingh, 2001). Thus, studies on identification of specific target(s) to regulate microglia activation and resultant production of neurotoxins are highly imperative. Our results, gp120-associated neurotoxicity was blocked by a specific $K_v1.3$ blocker MgTx, indicate that $K_v1.3$ expressed in microglia may function as a potential target for the development of therapeutic strategies for HAND and perhaps for other neurodegenerative disorders. We anticipate that blockade of $K_v1.3$ channels in microglia might attenuate microglia-associated neurotoxicity, resulting in the protection of neurons from HIV-associated challenge in the infected brain. It is worth pointing out that there may be side effects by systemic or intracranial administration of $K_v1.3$ blockers since small amounts of $K_v1.3$ are also expressed in several brain regions such as hippocampus, and pyriform cortex (Kues and Wunder, 1992). However, such potential side effects might be minimal as animals deficient in $K_v1.3$ exhibited only a heightened sense of smell and distinct structure alterations in the olfactory bulb (Fadool et al., 2004). Thus, the potential for development of specific $K_v1.3$ blockers to suppress microglia-associated neurotoxicity is optimistic.

In summary, the experimental data provide *in vitro* evidence that HIV-1gp120 enhances outward K^+ current in cultured rat microglia via CXCR4 → cAMP-dependent PKA signaling pathway. Gp120 elevates the levels of K_v channel expression and alters K_v channel biophysical properties. Biological significance of gp120 enhancement of microglia outward K^+ current was demonstrated by experimental results that blockade of microglia K_v channels by K_v channel blockers suppresses microglia-induced neurotoxicity. As such, the K_v channel

expressed in microglia may function as a potential target in the development of therapeutic strategies for neurodegenerative disorders by which the activated resident microglia play a critical role in the pathogenesis.

ACKNOWLEDGMENTS

The authors thank Mr. Bryan Katafiasz for reading the manuscript. The authors extend special thanks to Ms. Julie Ditter, Ms. Robin Taylor, and Ms. Johna Belling for their excellent administrative supports and to two anonymous reviewers for their critical criticisms and helpful comments.

REFERENCES

Aiello EA, Walsh MP, Cole WC. 1995. Phosphorylation by protein kinase A enhances delayed rectifier K+ current in rabbit vascular smooth muscle cells. Am J Physiol 268:H926–H934.

Albright AV, Shieh JT, Itoh T, Lee B, Pleasure D, O'Connor MJ, Doms RW, Gonzalez-Scarano F. 1999. Microglia express CCR5, CXCR4, and CCR3, but of these, CCR5 is the principal coreceptor for human immunodeficiency virus type 1 dementia isolates. J Virol 73:205–213.

Bachis A, Mocchetti I. 2004. The chemokine receptor CXCR4 and not the N-methyl-D-aspartate receptor mediates gp120 neurotoxicity in cerebellar granule cells. J Neurosci Res 75:75–82.

Beeton C, Wulff H, Standifer NE, Azam P, Mullen KM, Pennington MW, Kolski-Andreaco A, Wei E, Grino A, Counts DR, others. 2006. Kv1.3 channels are a therapeutic target for T cell-mediated autoimmune diseases. Proc Natl Acad Sci U S A 103:17414–17419.

Chandy KG, Gutman GA. 1995. Voltage-gated potassium channel genes. In: North RA, editor. Ligand and Voltage-gated Ion Channels. Bpca Raton, FL: CRC. pp 1–71.

Chandy KG, Wulff H, Beeton C, Pennington M, Gutman GA, Cahalan MD. 2004. K+ channels as targets for specific immunomodulation. Trends Pharmacol Sci 25:280–289.

Chung I, Schlichter LC. 1997. Regulation of native Kv1.3 channels by cAMP-dependent protein phosphorylation. Am J Physiol 273:C622–C633.

Dheen ST, Kaur C, Ling EA. 2007. Microglial activation and its implications in the brain diseases. Curr Med Chem 14:1189–1197.

Eder C. 1998. Ion channels in microglia (brain macrophages). Am J Physiol 275:C327–C342.

Eder C. 2005. Regulation of microglial behavior by ion channel activity. J Neurosci Res 81:314–321.

Eder C, Fischer HG, Hadding U, Heinemann U. 1995. Properties of voltage-gated currents of microglia developed using macrophage colony-stimulating factor. Pflugers Arch 430:526–533.

Elkabes S, Peng L, Black IB. 1998. Lipopolysaccharide differentially regulates microglial trk receptor and neurotrophin expression. J Neurosci Res 54:117–122.

Fadool DA, Tucker K, Perkins R, Fasciani G, Thompson RN, Parsons AD, Overton JM, Koni PA, Flavell RA, Kaczmarek LK. 2004. Kv1.3 channel gene-targeted deletion produces "Super-Smeller Mice" with altered glomeruli, interacting scaffolding proteins, and biophysics. Neuron 41:389–404.

Fakler B, Brandle U, Glowatzki E, Zenner HP, Ruppersberg JP. 1994. Kir2.1 inward rectifier K+ channels are regulated independently by protein kinases and ATP hydrolysis. Neuron 13:1413–1420.

Farber K, Kettenmann H. 2005. Physiology of microglial cells. Brain Res Brain Res Rev 48:133–143.

Fischer HG, Eder C, Hadding U, Heinemann U. 1995. Cytokine-dependent K+ channel profile of microglia at immunologically defined functional states. Neuroscience 64:183–191.

Fordyce CB, Jagasia R, Zhu X, Schlichter LC. 2005. Microglia Kv1.3 channels contribute to their ability to kill neurons. J Neurosci 25: 7139–7149.

Garden GA. 2002. Microglia in human immunodeficiency virus-associated neurodegeneration. Glia 40:240–251.

Gendelman HE, Eiden L, Epstein L, Grant I, Lipton SA, McArthur JC, Pomerantz R, Price R, Swindells S. 1997. Neuropathogenesis of HIV-1 Dementia: A Panel Discussion. New York: Chapman & Hall.

Genis P, Jett M, Bernton EW, Boyle T, Gelbard HA, Dzenko K, Keane RW, Resnick L, Mizrachi Y, Volsky DJ, others. 1992. Cytokines and arachidonic metabolites produced during human immunodeficiency virus (HIV)-infected macrophage-astroglia interactions: implications for the neuropathogenesis of HIV disease. J Exp Med 176:1703–1718.

Glass JD, Wesselingh SL. 2001. Microglia in HIV-associated neurological diseases. Microsc Res Tech 54:95–105.

Hesselgesser J, Taub D, Baskar P, Greenberg M, Hoxie J, Kolson DL, Horuk R. 1998. Neuronal apoptosis induced by HIV-1 gp120 and the chemokine SDF-1 alpha is mediated by the chemokine receptor CXCR4. Curr Biol 8:595–598.

Kaul M, Garden GA, Lipton SA. 2001. Pathways to neuronal injury and apoptosis in HIV-associated dementia. Nature 410:988–994.

Kennelly PJ, Krebs EG. 1991. Consensus sequences as substrate specificity determinants for protein kinases and protein phosphatases. J Biol Chem 266:15555–15558.

Kielian T. 2004. Microglia and chemokines in infectious diseases of the nervous system: Views and reviews. Front Biosci 9:732–750.

Knaus HG, Koch RO, Eberhart A, Kaczorowski GJ, Garcia ML, Slaughter RS. 1995. [125I]margatoxin, an extraordinarily high affinity ligand for voltage-gated potassium channels in mammalian brain. Biochemistry 34:13627–13634.

Koenig S, Gendelman HE, Orenstein JM, Dal Canto MC, Pezeshkpour GH, Yungbluth M, Janotta F, Aksamit A, Martin MA, Fauci AS. 1986. Detection of AIDS virus in macrophages in brain tissue from AIDS patients with encephalopathy. Science 233:1089–1093.

Kotecha SA, Schlichter LC. 1999. A Kv1.5 to Kv1.3 switch in endogenous hippocampal microglia and a role in proliferation. J Neurosci 19:10680–10693.

Kues WA, Wunder F. 1992. Heterogeneous Expression Patterns of Mammalian Potassium Channel Genes in Developing and Adult Rat Brain. Eur J Neurosci 4:1296–1308.

Lavi E, Strizki JM, Ulrich AM, Zhang W, Fu L, Wang Q, O'Connor M, Hoxie JA, Gonzalez-Scarano F. 1997. CXCR-4 (Fusin), a co-receptor for the type 1 human immunodeficiency virus (HIV-1), is expressed in the human brain in a variety of cell types, including microglia and neurons. Am J Pathol 151:1035–1042.

Lipton SA, Gendelman HE. 1995. Seminars in medicine of the Beth Israel Hospital, Boston Dementia associated with the acquired immunodeficiency syndrome [see comments]. N Engl J Med 332:934–940.

Menteyne A, Levavasseur F, Audinat E, Avignone E. 2009. Predominant functional expression of Kv1.3 by activated microglia of the hippocampus after Status epilepticus. PLoS One 4:e6770

Meucci O, Fatatis A, Simen AA, Bushell TJ, Gray PW, Miller RJ. 1998. Chemokines regulate hippocampal neuronal signaling and gp120 neurotoxicity. Proc Natl Acad Sci U S A 95:14500–14505.

Miwa T, Furukawa S, Nakajima K, Furukawa Y, Kohsaka S. 1997. Lipopolysaccharide enhances synthesis of brain-derived neurotrophic factor in cultured rat microglia. J Neurosci Res 50:1023–1029.

Newell EW, Schlichter LC. 2005. Integration of K+ and Cl- currents regulate steady-state and dynamic membrane potentials in cultured rat microglia. J Physiol 567:869–890.

Norenberg W, Gebicke-Haerter PJ, Illes P. 1994. Voltage-dependent potassium channels in activated rat microglia. J Physiol 475:15–32.

Pannasch U, Farber K, Nolte C, Blonski M, Yan Chiu S, Messing A, Kettenmann H. 2006. The potassium channels Kv1.5 and Kv1.3 modulate distinct functions of microglia. Mol Cell Neurosci 33:401–411.

Perozo E, Bezanilla F, Dipolo R. 1989. Modulation of K channels in dialyzed squid axons. ATP-mediated phosphorylation. J Gen Physiol 93: 1195–1218.

Schilling T, Quandt FN, Cherny VV, Zhou W, Heinemann U, Decoursey TE, Eder C. 2000. Upregulation of Kv1.3 K(+) channels in microglia deactivated by TGF-beta. Am J Physiol Cell Physiol 279:C1123–C1134.

Toggas SM, Masliah E, Rockenstein EM, Rall GF, Abraham CR, Mucke L. 1994. Central nervous system damage produced by expression of the HIV-1 coat protein gp120 in transgenic mice. Nature 367:188–193.

Walz W, Bekar LK. 2001. Ion channels in cultured microglia. Microsc Res Tech 54:26–33.

Cellular & Molecular Immunology (2011) 8, 305–314

www.nature.com/cmi

RESEARCH ARTICLE

The increase in surface CXCR4 expression on lung extravascular neutrophils and its effects on neutrophils during endotoxin-induced lung injury

Mitsuhiro Yamada[1], Hiroshi Kubo[2], Seiichi Kobayashi[3], Kota Ishizawa[2], Mei He[2], Takaya Suzuki[2], Naoya Fujino[2], Hiroyuki Kunishima[1], Masamitsu Hatta[1], Katsushi Nishimaki[4], Tetsuji Aoyagi[4], Kouichi Tokuda[4], Miho Kitagawa[4], Hisakazu Yano[5], Hirokazu Tamamura[6], Nobutaka Fujii[7] and Mitsuo Kaku[1,4]

Inflammatory stimuli, such as a microbes or lipopolysaccharides, induce a rapid release of neutrophils from the bone marrow and promote neutrophil migration into inflamed sites to promote host defense. However, an excess accumulation and retention of neutrophils in inflamed tissue can cause severe tissue injuries in the later stages of inflammation. Recent studies have reported that both CXCL12 levels in injured lungs and its receptor, CXCR4, on accumulated neutrophils in injured lungs, increased; furthermore, these studies showed that the CXCL12/CXCR4 signaling pathway participated in neutrophil accumulation in the later stages of lipopolysaccharide (LPS)-induced lung injury. However, the mechanisms underlying this increase in surface CXCR4 expression in neutrophils remain unclear. In this study, we found that surface CXCR4 expression increased in extravascular, but not intravascular, neutrophils in the lungs of LPS-induced lung injury model mice. Furthermore, *ex vivo* studies revealed that CXCL12 acted not only as a chemoattractant, but also as a suppressor of cell death for the lung neutrophils expressing CXCR4. Sulfatide, one of the native ligands for L-selectin, induced the increase of surface CXCR4 expression on isolated circulating neutrophils, suggesting that the activation of L-selectin may be involved in the increase in surface CXCR4. Our findings show that surface CXCR4 levels on neutrophils increase after extravasation into injured lungs, possibly through the activation of L-selectin. The CXCL12/CXCR4 signaling pathway plays an important role in the modulation of neutrophil activity during acute lung injury, not only by promoting chemotaxis but also by suppressing cell death.
Cellular & Molecular Immunology (2011) **8**, 305–314; doi:10.1038/cmi.2011.8; published online 4 April 2011

Keywords: CXCL12; CXCR4; lipopolysaccharides; lung injury; neutrophils

INTRODUCTION

During acute inflammation, neutrophils are released from the bone marrow and migrate into inflamed tissues.[1,2] In inflamed tissues, neutrophils extravasate from blood vessels to the site of tissue injury or infection. These extravasated neutrophils play an important role in host defense against pathogenic microorganisms, though the excess accumulation and activation of neutrophils can cause severe tissue injury. Therefore, the apoptosis of neutrophils and the proper processing of apoptotic neutrophils by macrophage phagocytosis are important for the resolution of inflammation to prevent tissue injury. It is well established that inflammatory cytokines (including TNF-α[3] and IL-1[4]) and neutrophil attractant CXC chemokines[5–7] are critically involved in the accumulation of neutrophils within injured tissues during the acute phase of inflammation. However, the mechanisms of neutrophil retention and withdrawal during the later phase of inflammation are not well understood and are still being investigated.

The accumulated evidence published thus far suggests that CXC chemokine CXCL12/stromal cell-derived factor-1, which was first described as a strong chemotactic factor for lymphocytes,[8–11] contributes to the control of the neutrophil life cycle through the activation of CXCR4. It has been reported that the CXCL12/CXCR4 signaling system plays an important role in the regulation of neutrophil homeostasis, including both the release of neutrophils from bone marrow into blood[12–15] and the homing of the circulating neutrophils to the bone marrow.[14,16] In addition to the evidence supporting the role of

[1]Department of Regional Cooperation for Infectious Diseases, Tohoku University Graduate School of Medicine, Sendai, Miyagi, Japan; [2]Department of Advanced Preventive Medicine for Infectious Disease, Tohoku University Graduate School of Medicine, Sendai, Miyagi, Japan; [3]Department of Respiratory Medicine, Japanese Red-Cross Ishinomaki Hospital, Ishinomaki, Miyagi, Japan; [4]Department of Infection Control and Laboratory Diagnostics, Tohoku University Graduate School of Medicine, Sendai, Miyagi, Japan; [5]Department of Clinical Microbiology with Epidemiological Research & Management and Analysis of Infectious Diseases, Tohoku University Graduate School of Medicine, Sendai, Miyagi, Japan; [6]Institute of Biomaterials and Bioengineering, Tokyo Medical and Dental University, Chiyoda-ku, Tokyo, Japan and [7]Graduate School of Pharmaceutical Sciences, Kyoto University, Kyoto, Japan
Correspondence: Dr H Kubo, Department of Advanced Preventive Medicine for Infectious Disease, Tohoku University Graduate School of Medicine, 2-1 Seiryoumachi, Aobaku, Sendai 980-8575, Japan.
E-mail: hkubo@med.tohoku.ac.jp
Received 9 December 2010; revised 8 February 2011; accepted 23 February 2011

CXCL12/CXCR4 in modulating neutrophil homeostasis, we and other investigators previously reported that both CXCL12 levels in the injured lungs and surface CXCR4 protein on accumulated neutrophils were increased; furthermore, the *in vivo* administration of an anti-CXCL12 blocking antibody suppressed airspace neutrophilia in the lungs in the later stages of lipopolysaccharide (LPS)-induced lung injury.[17–19] These findings suggested that this chemokine participated in the accumulation of neutrophils in the injured tissue, particularly in the later stages of inflammation. However, the mechanisms underlying the increase in surface CXCR4 expression on neutrophils during LPS-induced lung injury and the CXCL12-promoted accumulation of neutrophils remain unclear.

In this study, we investigated when and how surface CXCR4 expression levels increased on neutrophils in the lungs during LPS-induced lung injury. We further examined the effects of CXCL12 on isolated neutrophils to evaluate how this chemokine contributes to neutrophil accumulation in the injured tissue. In our investigation of the mechanism underlying the increase in surface CXCR4 expression levels, we focused on L-selectin because previous reports have shown that the activation of L-selectin induced the expression of surface CXCR4 in both human and mouse lymphocytes;[20,21] furthermore, the shedding of L-selectin, which resulted from the activation of L-selectin by its ligands,[22] was observed in extravasated neutrophils in inflamed tissues of mice.[23,24]

MATERIALS AND METHODS

Animals

C57BL/6J mice were purchased from CLEA Japan Inc. (Tokyo, Japan). All mice were 7- to 8-week-old males and were housed under specific pathogen-free conditions for 1 week prior to experimental use. All animal experiments were permitted by the Institutional Animal Care and Use Committee of the Tohoku University Environmental and Safety Committee and were performed in accordance with the Regulations for Animal Experiments and Related Activities at Tohoku University.

Reagents

The reagents used in this study were obtained from the following sources: mouse monoclonal anti-CXCL12 blocking antibody was purchased from R&D Systems (Minneapolis, MN, USA); control mouse immunoglobulin G1 (IgG1) was purchased from Sigma (St Louis, MO, USA); a specific CXCR4 antagonist, 4F-benzoyl-TE14011, was synthesized as previously described;[25,26] a rabbit anti-mouse CXCL12 antibody was purchased from BioVision (Mountain View, CA, USA) for immunohistochemical experiments; mouse monoclonal anti-mouse/human CXCL12 antibody was purchased from R&D Systems for immunoblotting analysis; phycoerythrin (PE)-conjugated rat anti-mouse CXCR4 monoclonal antibody (clone 2B11/CXCR4) and an isotype control antibody (clone A95-1), PE-conjugated rat IgG2b), fluorescein isothiocyanate (FITC)-conjugated rat anti-mouse Ly-6G monoclonal antibody (clone 1A8) and purified rat anti-mouse CD16/CD32 (Fcγ III/II receptor) monoclonal antibody (clone 2.4G2, Mouse BD Fc Block) were purchased from BD Pharmingen (San Diego, CA, USA); FITC-conjugated anti-mouse neutrophil antibody (clone 7/4) was purchased from Serotec (Raleigh, NC, USA); Alexa Fluor 647-conjugated anti-mouse Ly-6G (Gr-1) monoclonal antibody (clone RB6-8C5), 7-aminoactinomycin D (7-AAD) viability staining solution and an Annexin V apoptosis detection kit APC were purchased from eBioscience (San Diego, CA, USA); Alexa Fluor 647 anti-mouse CD62L antibody and Alexa Fluor 647 rat IgG2a, κ isotype control antibody were purchased from Biolegend (San Diego, CA, USA); recombinant mouse CXCL12α was purchased from R&D Systems; sulfatide sodium salt from bovine spinal cord was purchased from Wako Chemicals (Tokyo, Japan); TRIzol reagent was purchased from Invitrogen (Carlsbad, CA, USA); anti-p44/42 MAPK (ERK1/2) rabbit monoclonal antibody, anti-phospho-p44/42 MAPK (ERK1/2, Thr202 and Tyr204) rabbit monoclonal antibody, anti-Akt rabbit monoclonal antibody, anti-phospho-Akt (Thr308) rabbit monoclonal antibody, goat anti-rabbit IgG, HRP-linked antibody, cell lysis buffer, U0126 (MEK1/2 inhibitor) and LY294002 (PI3 kinase inhibitor) were purchased from Cell Signaling Technology (Danvers, MA, USA).

LPS-induced lung injury

LPS from *Escherichia coli* serotype 055:B5 was obtained from Sigma. Mice were anesthetized by ketamine hydrochloride. While anesthetized, mice intranasally inhaled LPS (20 μg/mouse in phosphate-buffered saline (PBS)) that was placed on one nostril. Control mice received only PBS.

Preparation of single lung cells from lungs

Mice received an overdose of inhaled halothane, and their lungs were perfused with PBS *via* the right ventricles. PBS-perfused lungs were isolated with other mediastinal organs. Dispase II solution was instilled into the lungs through the trachea, which was ligated with a silk suture. After incubation at 37 °C for 50 min, the lungs were separated from the other mediastinal organs. The lungs were then thoroughly minced and digested in PBS with 0.1% collagenase, 0.01% deoxyribonuclease I and 5-mM $CaCl_2$ at 37 °C for 20 min. The cells were then suspended in red blood cell lysing buffer to remove red blood cells and subsequently washed with PBS. The cells were then centrifuged and resuspended in PBS.

Evaluation of surface CXCR4 expression on neutrophils

The surface CXCR4 expression levels of neutrophils isolated from bone marrow, circulating blood, single lung cell suspensions and BAL fluid were evaluated. Mouse neutrophils were identified by their forward scatter and side scatter characteristics and positive Ly-6G staining. The samples were stained with a PE-labeled anti-CXCR4 antibody or a PE-labeled isotype-matched control antibody and an FITC-labeled anti-Ly6G (1A8) antibody. Dead cells were excluded based on 7-AAD staining. The samples were analyzed using a FACSCalibur flow cytometer (BD Biosciences, San Jose, CA, USA).

Identification of intravascular and extravascular neutrophils in the lungs

The identification of intravascular and extravascular neutrophils in the lungs was performed as previously described with some modifications.[27] An Alexa Fluor 647-conjugated anti-mouse Ly-6G (Gr-1) antibody (1 μg) was injected intravenously and allowed to circulate for 5 min. After 5 min, the mice were killed. The lungs were then digested as described above in the presence of an excess of unlabeled anti-mouse Gr-1 antibody to prevent possible binding of Alexa Fluor 647-conjugated anti-Gr-1 antibody to extravascular neutrophils. The lung cell suspensions were then stained with an FITC-conjugated anti-mouse neutrophil antibody (7/4). Intravascular ($7/4^+Gr\text{-}1^+$) and extravascular ($7/4^+Gr\text{-}1^-$) neutrophil populations were assessed using flow cytometry.

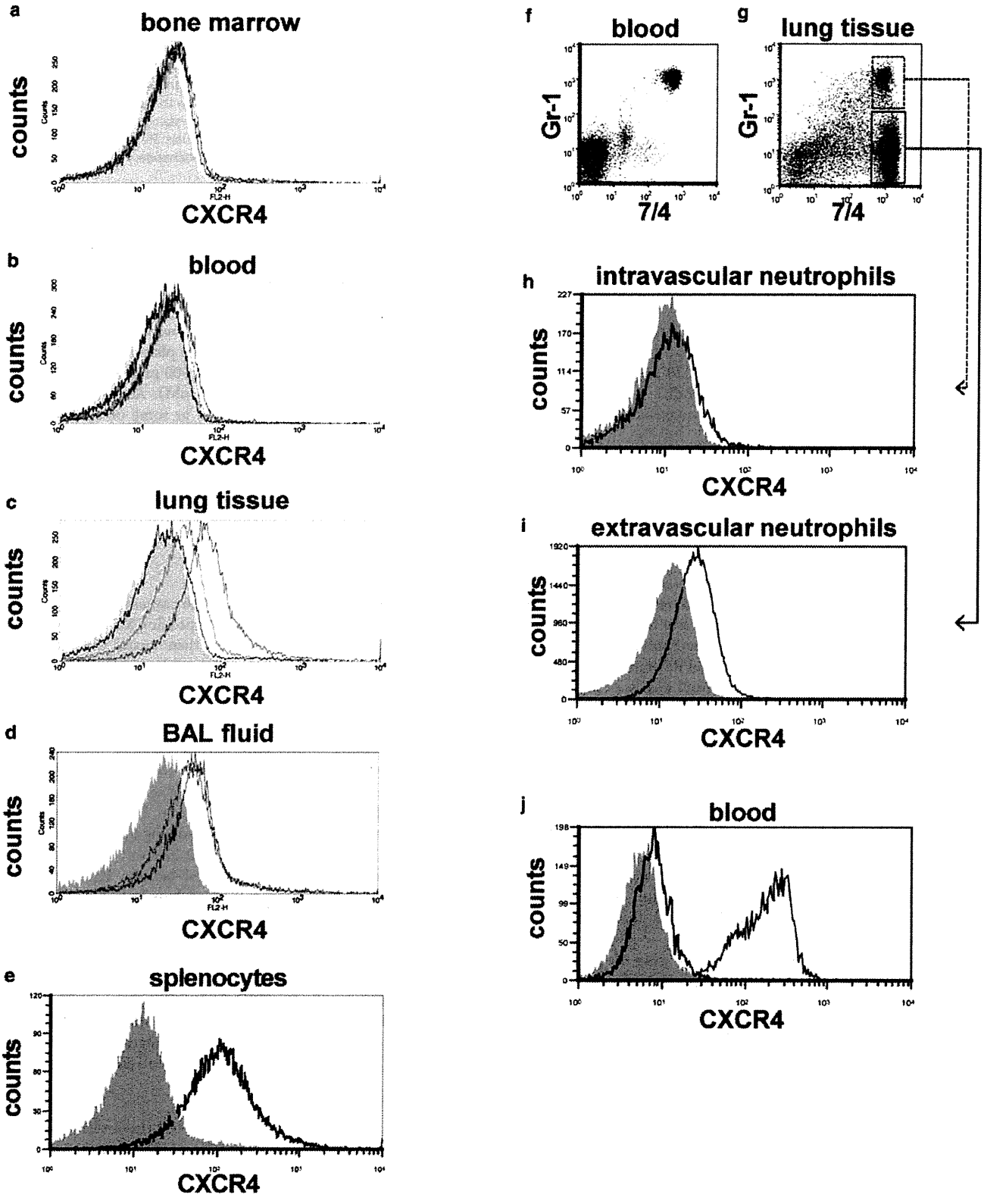

Figure 1 Surface CXCR4 expression increased in extravascular neutrophils in the mouse lungs during LPS-induced lung injury. (**a**–**e**) Flow cytometric analyses were performed to determine the surface CXCR4 expression levels of neutrophils isolated from bone marrow (**a**), peripheral blood (**b**), lung tissue (**c**) and BAL fluid (**d**). Neutrophils were analyzed before LPS administration (black line) and at 6 h (red line) and 24 h (blue line) afterward. The filled images show the staining using an

isotype-matched control antibody. We were unable to analyze the surface CXCR4 expression levels of neutrophils isolated from BAL fluid before LPS administration because there were an insufficient number of neutrophils in these samples. Splenocytes from untreated control mice were used as a positive control for CXCR4 staining (**e**). (**f–i**) The surface CXCR4 expression levels of intravascular neutrophils (**g**; GR-1$^+$7/4$^+$) and extravascular neutrophils (**g**; GR-1$^-$7/4$^+$) in the lungs at 24 h during LPS-induced lung injury were examined. Note almost all circulating neutrophils (7/4$^+$ cells) in blood were stained with Gr-1 5 min after antibody injection (**f**). The blue lines show the surface CXCR4 expression levels of intravascular neutrophils (**h**) or extravascular neutrophils (**i**). The filled images show the staining using an isotype-matched control antibody. (**h**) The levels of intracellular CXCR4 (blue line) in neutrophils isolated from mouse blood were analyzed by staining with permeabilization. The filled image shows the staining using an isotype-matched control antibody. The black line shows the surface CXCR4 expression levels. Representative histograms or dot plots from one of three experiments that showed similar results are presented. BAL, bronchoalveolar lavage; LPS, lipopolysaccharide.

In vivo blocking the CXCL12/CXCR4 signaling pathway using a specific CXCR4 antagonist

A specific CXCR4 antagonist (4F-benzoyl-TE14011) was used for *in vivo* inhibition of the CXCL12/CXCR4 signaling pathway as described previously.[28] Briefly, 4F-benzoyl-TE14011 was dissolved in PBS and subcutaneously administered using ALZET osmotic pumps (Durect Corp., Cupertino, CA, USA) that were implanted dorsally under the skin 1 day before administration of LPS. 4F-benzoyl-TE14011 was infused at a rate of 120 μg/day for 3 days after implantation. For the control study, ALZET osmotic pumps filled with the same volume of PBS were subcutaneously implanted in the same manner.

Bronchoalveolar lavage (BAL)

First, mice were killed by administering an overdose of halothane. Lavage tubes were then implanted into the mice according to the following procedure: a median sternotomy was performed, the trachea were dissected and isolated from the underlying soft tissues and a 0.8-mm lavage tube was inserted through a small incision in the trachea. BAL was performed by instilling 0.5 ml of ice cold PBS into the lungs and then gently aspirating the fluid. BAL was then repeated two times using fresh 0.5-ml aliquots of PBS. These three fluid samples were pooled and centrifuged. Cell counts and differentials were then performed. BAL protein in cell-free BAL fluid was assayed as an index of lung injury and capillary leakage. Protein quantification was performed using a BCA Protein Assay Reagent Kit (Pierce Biotechnology Inc., Rockford, IL, USA).

Histological analysis

The lungs were fixed by inflation with 10% neutral-buffered formalin at a transpulmonary pressure of 20 cm H_2O, embedded in paraffin and cut into 5-μm thick sections. Sections were stained with hematoxylin and eosin for histological assessment. Images were taken with Nikon Eclipse E80i Microscope (Nikon, Tokyo, Japan). These images were analyzed using ImageJ software (National Institutes of Health, Bethesda, MD, USA).

The lung injury scores were calculated using the previously published scoring system.[29] Two sections per animal were scored independently. Alveolar wall thickness was quantified in a blinded fashion by measuring of all septa along a crosshair placed on each image. At least 200 septa per animal were measured. The number of emigrated neutrophils was quantified by counting the number neutrophils present within all alveolar spaces in randomly selected fields. At least 200 alveolar spaces were counted.

Isolation of lung neutrophils

Neutrophils were separated from bone marrow cells, circulating blood leukocytes and single lung cell suspensions using an anti-Ly6G (1A8) MicroBead Kit (Miltenyi Biotec, Bergisch Gladbach, Germany) according to the manufacturer's protocol. The purity of the isolated neutrophils was evaluated using both microscopic and flow cytometric analyses and was determined to be greater than 98%.

Neutrophil migration assay

Neutrophils were placed on a modified Boyden chamber with 3-μm pores (Chemotaxcell; Kurabo Industries Ltd, Osaka, Japan) to evaluate the migration stimulating activity of CXCL12. Splenocytes, which can migrate toward CXCL12,[26] were used as a positive control. A total of 5×10^5 neutrophils or splenocytes in 200 μl of RPMI 1640 medium containing 0.25% bovine serum albumin were placed in the upper chambers. The upper chambers were then placed in individual wells of a 24-well cell culture plate containing 500 μl of assay buffer either with or without mouse CXCL12α (50 nM). An equal number of neutrophils or splenocytes were added to some of the lower wells without a top chamber to provide a standard count of total cells. In some experiments, the cells were pre-incubated with 100-nM 4F-benzoyl-TE14011 at 37 °C for 30 min. The chambers were then incubated for 2 h at 37 °C. The cells in the lower chamber were collected, and the percentage of migration was determined from the original cell input.

Cell death analysis

Lung neutrophils (2×10^6) in RPMI 1640 containing 10% FCS were either untreated or preincubated with a specific CXCR4 antagonist for 1 h at 37 °C. The neutrophils were then mixed with 100 ng/ml CXCL12α alone or in combination with a MEK1/2 inhibitor (U0126, 1 μM) or a PI3K inhibitor (LY294002, 10 μM) and incubated for an additional 24 h at 37 °C. After this incubation, the neutrophils were counted and the percentage of dead cells was calculated using trypan blue staining. Neutrophils were also stained with Annexin V and 7-AAD, and then analyzed using a FACSCalibur flow cytometer.

Western blotting

Lung neutrophils isolated from the injured lung were left untreated or incubated at 37 °C with 100 ng/ml CXCL12α for 30 s. Some neutrophils were pre-incubated with 100-nM 4F-benzoyl-TE14011 at 37 °C for 30 min. Cells were lysed in 1× cell lysis buffer (Cell Signaling Technology). Whole-cell lysate was run on an any kD Mini-PROTEAN TGX Precast SDS-PAGE gel (Bio-Rad, Hercules, CA, USA) and the proteins were transferred by electroblotting onto polyvinylidene fluoride membrane (Invitrogen). The blots were probed with antibodies specific for ERK1/2 phosphorylation at Thr202 and Tyr204 or Akt phosphorylation at Thr 308. Membranes were stripped with Restore Western Blot Stripping Buffer (Thermo Fisher Scientific, Rockford, IL, USA) and then reblotted with anti-ERK1/2 or anti-Akt.

L-selectin stimulation

Neutrophils were resuspended in RPMI 1640 (Invitrogen) with 0.1% bovine serum albumin (Sigma). The neutrophils were then incubated with sulfatide at a final concentration of 100 μg/ml for 1 h at 37 °C.

Data presentation and statistical analysis

Unless otherwise noted, all data presented are expressed as mean± standard error of the mean (s.e.m.). Statistical analyses were performed using Statistica software (StatSoft Inc., Tulsa, OK, USA).

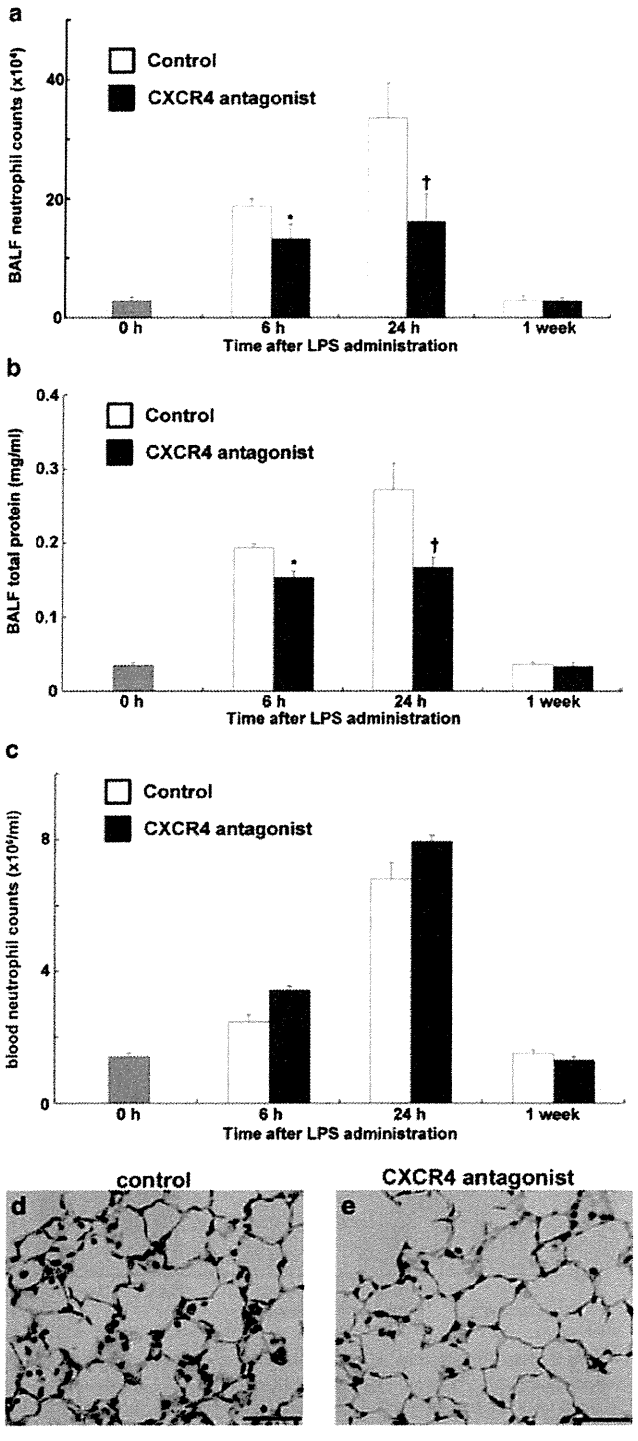

Figure 2 Blocking the CXCL12/CXCR4 signaling pathway inhibited neutrophil migration into the lung air space and the increase of lung permeability during LPS-induced lung injury. (**a–c**) Neutrophil counts (**a**), total protein concentration (**b**) in the BALF and neutrophil counts in the circulating blood (**c**) were determined in C57BL/6 mice treated with either PBS (white) or a CXCR4 antagonist (black) at indicated time points during LPS-induced lung injury. A total of six mice were used in each group. Values represent mean±s.e.m. **P*<0.01, †*P*<0.05, versus PBS control mice using ANOVA with Scheffé's *post hoc* test. (**d**, **e**) Histological evaluation of the treatment with a CXCR4 antagonist on LPS-induced lung injury. Representative images of hematoxylin and eosin stained lung tissue sections from PBS- (**d**) or CXCR4 antagonist-treated (**e**) mice at 24 h during LPS-induced lung injury. Scale bar=50 μm. BALF, bronchoalveolar lavage fluid; LPS, lipopolysaccharide; PBS, phosphate-buffered saline.

Data were assessed for significance by ANOVA with Scheffé's *post hoc* method for multiple comparisons. Statistical significance was defined as $P<0.05$.

RESULTS

The expression of surface CXCR4 increased on extravascular neutrophils in the mouse lungs during LPS-induced lung injury

Neutrophils in bone marrow, peripheral blood and lung digests from untreated control mice expressed very low levels of surface CXCR4 (Figure 1a–c, black lines). Surface expression of CXCR4 did not clearly increased in neutrophils from the bone marrow or peripheral blood at 6 and 24 h after LPS instillation (Figure 1a and b, red and blue lines, respectively). However, neutrophils from lung digests and BAL fluids exhibited a significant increase in surface CXCR4 expression at both 6 and 24 h during LPS-induced lung injury (Figure 1c and d, red and blue lines, respectively). To investigate whether a subset of neutrophils with higher surface CXCR4 expression in the blood emigrates into the lungs or if neutrophil surface CXCR4 expression increases after the cells emigrate into the lungs, we examined the surface CXCR4 expression of both intravascular and extravascular neutrophils in the lungs during LPS-induced lung injury. We first labeled intravascular neutrophils *in vivo* by the intravascular administration of the Alexa 647-conjugated anti-mouse Gr-1 antibody and labeled all neutrophils in the lung digest using the FITC-conjugated anti-mouse 7/4 antibody (Figure 1f and g, also see the section on 'Materials and methods'). Almost all circulating neutrophils in blood were stained with Gr-1 5 min after antibody injection (Figure 1f). Extravascular neutrophils, which were labeled with the anti-7/4 but not the anti-Gr-1 antibody (Figure 1g), exhibited clearly higher surface CXCR4 expression levels (Figure 1i) compared to intravascular neutrophils (Figure 1h). As previously reported in humans,[16] intracellular staining revealed that the levels of CXCR4 expression were high in the intracellular compartments of neutrophils isolated from mouse blood (Figure 1j), suggesting that translocation of CXCR4 to the cell surface occurred in the neutrophils isolated from injured lungs. Taken together, these findings suggested that the cell surface CXCR4 expression levels increased after these cells emigrated into the lungs and extravasated during LPS-induced lung injury.

Blocking the CXCL12/CXCR4 signaling pathway inhibited neutrophil accumulation into the air space and attenuated the increase in lung permeability during LPS-induced lung injury.

Previous reports by our group and other investigators have shown that CXCL12 levels are upregulated in injured lungs and that *in vivo* administration of anti-CXCL12 blocking antibodies suppresses airspace neutrophilia in the lungs at the later stages of LPS-induced lung injury,[17–19] suggesting that the increase of surface CXCR4 expression on lung extravasated neutrophils cooperates with the increase of CXCL12 in the lungs to facilitate the accumulation of neutrophils. To confirm the *in vivo* role of the CXCL12/CXCR4 signaling system in the pathogenesis of acute lung injury, we administrated a specific CXCR4 antagonist to block the activation of CXCR4. Because it has been reported that single-dose administration of a CXCR4 antagonist rapidly induces neutrophilia,[12,30,31] we administrated the antagonist continuously using an osmotic pump as previously we did.[28] We compared white blood cell and neutrophil count between

Table 1 Histopathological lung injury score, interalveolar septal thickness and the number of neutrophils in alveolar spaces in mice at 24 h during LPS-induced lung injury

Measure	*Untreated control*	*LPS and PBS*	*LPS and CXCR4 antagonist*
Lung injury score	1.1±0.1	3.3±0.1	2.5±0.2*
Septal thickness (μm)	1.6±0.1	2.9±0.1	2.5±0.1*
No. of neutrophils in 100 alveoli	1.2±0.3	68.3±4.6	48.5±2.9*

Abbreviations: LPS, lipopolysaccharide; PBS, phosphate-buffered saline.
Data are represented as mean±s.e.m. $n=6$ per group.
*$P<0.01$ versus LPS and PBS group.

subcutaneous single-dose and continuous dosing administration of 4F-benzoyl-TE14011 in uninjured mice. As previously reported in human,[30,31] single-dose administration of 4F-benzoyl-TE14011 caused the significant neutrophilia with a peak increase at 6 h (Supplementary Table 1). However, continuous dosing administration did not cause the significant neutrophilia (Supplementary Table 1). Continuous administration of the antagonist also did not result in significant neutrophilia in comparison with control mice during LPS-induced lung injury (Figure 2c). The number of the neutrophils (Figure 2a) and the protein concentration (Figure 2b) in the BAL fluid were significantly reduced in CXCR4 antagonist treated mice at 6 and 24 h during LPS-induced lung injury in comparison with the control mice. Histological assessment also revealed that the treatment with a CXCR4 antagonist attenuated the lung injury induced by LPS at 24 h (Figure 2e and c and Table 1). These findings confirmed that both CXCL12 and its receptor CXCR4 contribute to neutrophil accumulation in the air space and an increase in lung permeability during LPS-induced lung injury.

Neutrophils isolated from injured lungs exhibited migratory activity toward CXCL12

To elucidate the role of CXCR4 in the accumulation of neutrophils in the injured lung, we examined whether lung neutrophils responded to and showed the migratory activity toward CXCL12. Isolated neutrophils from the LPS-instilled mice were placed in modified Boyden chambers, and CXCL12 was added to the chambers as a chemoattractant. Splenocytes from untreated control mice were used as a positive control because splenocytes expressed high levels of surface CXCR4 (Figure 1e). Neutrophils isolated from the bone marrow or peripheral blood exhibited no migratory response toward CXCL12 (Figure 3). In contrast, neutrophils isolated from lung digests and BAL fluids exhibited migratory responses to CXCL12 (Figure 3). Furthermore, this migratory response to CXCL12 was blocked by a specific CXCR4 antagonist. These *ex vivo* findings demonstrated that the accumulated lung neutrophils expressing high surface levels of CXCR4 exhibited migratory activity toward CXCL12, whereas bone marrow and peripheral blood neutrophils, which express very low surface levels of CXCR4, did not respond to CXCL12.

Activation of CXCR4 by CXCL12 attenuated cell death of isolated neutrophils from the injured lungs

The observation that blocking the CXCL12/CXCR4 pathway decreased the number of neutrophils in the air space suggests the involvement in neutrophil recruitment during LPS-induced lung injury. However, in contrast to the enhanced migratory activity toward CXCL12 observed in the accumulated lung neutrophils, the blood neutrophils, which expressed very low levels of CXCR4 (Figure 1), did not exhibit a migratory response to CXCL12 (Figure 3). This suggested that the CXCL12/CXCR4 pathway was not critically involved in the recruitment of neutrophils, at least from circulating blood into the injured lungs. It has been reported that CXCR4 activation by CXCL12 suppressed cell death of $CD34^+$ hematopoietic cells[32] and $CD4^+$ T cells.[33] To investigate whether the CXCL12/CXCR4 pathway contributes to the accumulation of neutrophils in the injured lung by suppressing the neutrophil death, we examined the role of CXCL12 in suppressing cell death of the lung neutrophils. We performed trypan blue staining to assess cell death after *ex vivo* culture either with or without CXCL12. The administration of CXCL12 decreased cell death levels of the neutrophils (Figure 4a). This protective effect of CXCL12 against cell death was blocked by the administration of a specific CXCR4 antagonist (Figure 4b–d). We further performed Annexin V and 7-AAD staining to assess apoptosis levels after culture. The incidences of both early apoptotic cells and late apoptotic/necrotic cells were reduced by CXCL12. This protective effect against apoptosis was also blocked by a CXCR4 antagonist (Figure 4b–d).

We then investigated the mechanisms for how CXCL12/CXCR4 signaling protects neutrophils from apoptosis. We focused on both ERK and PI3K/Akt signaling pathways because it has been reported that CXCL12/CXCR4 signaling protects T cells,[33] $CD34^+$

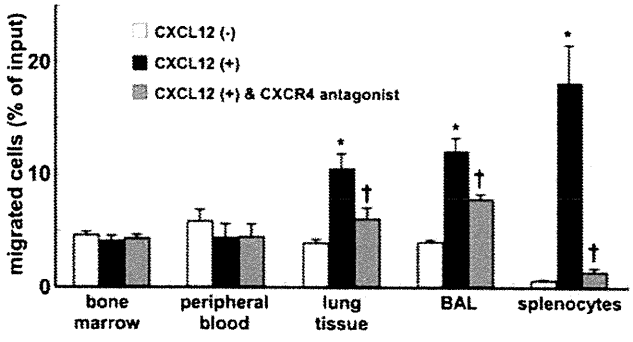

Figure 3 Neutrophils that accumulated in the mouse lungs during LPS-induced lung injury showed migratory responses to CXCL12. Neutrophils were isolated from the bone marrow, blood, lung tissue and BAL fluid at 24 h during LPS-induced lung injury. Cell migration assays assessing the migration of neutrophils toward CXCL12 were performed *in vitro* using chemotaxis chambers. Splenocytes from untreated control mice were used as a positive control because splenocytes expressed high levels of surface CXCR4 (Figure 1e). Levels of neutrophil or splenocyte migration in the absence of CXCL12, the presence of CXCL12, or after pretreatment with a CXCR4 antagonist in the presence of CXCL12, are depicted by the white, black and gray bars, respectively. The data shown represent the percentage of migration. The results were obtained from five mice in each group. Values represent mean±s.e.m. *$P<0.01$ versus CXCL12 (−) control group and †$P<0.01$ versus CXCL12 (+) group using ANOVA with Scheffé's *post hoc* test. BAL, bronchoalveolar lavage.

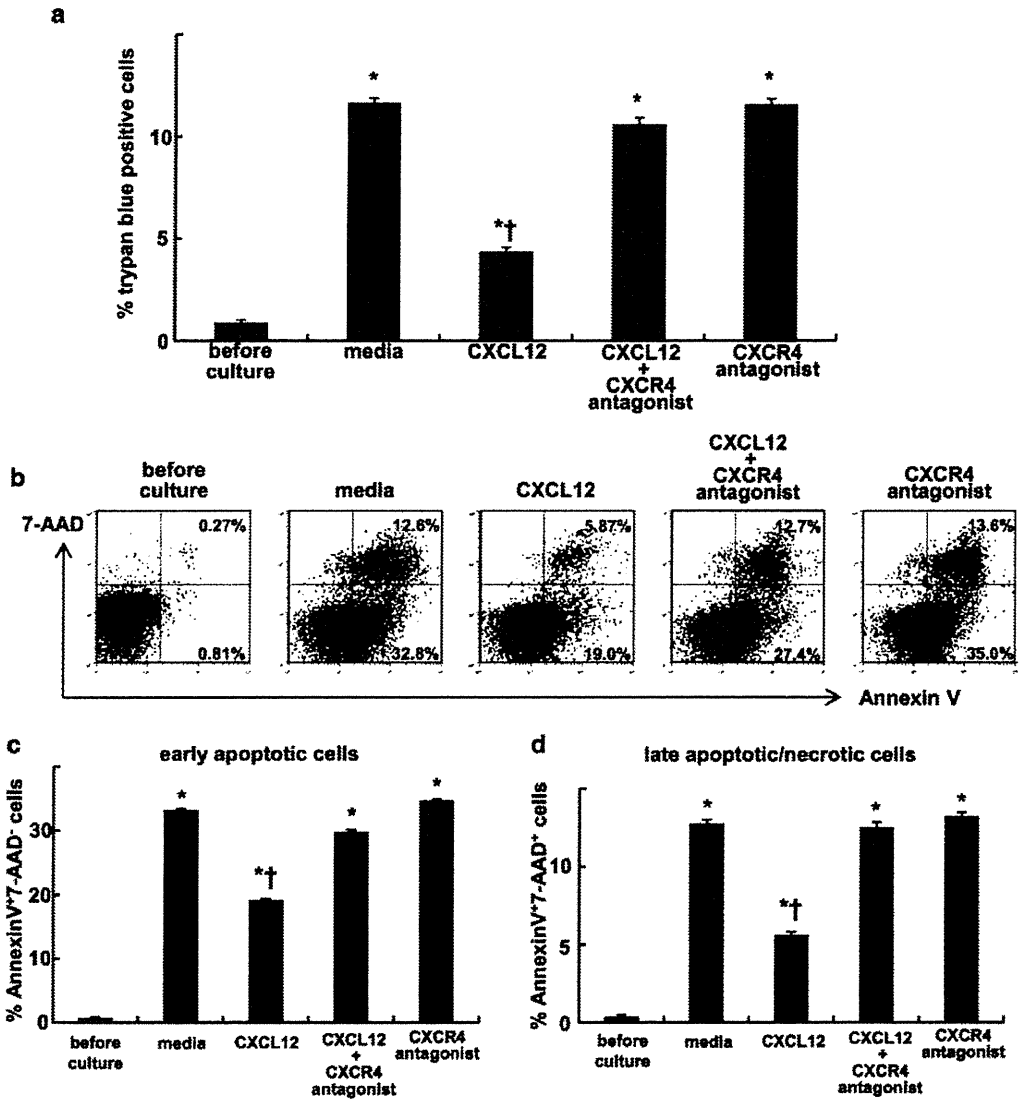

Figure 4 CXCR4 activation by CXCL12 attenuated the cell death of mouse neutrophils isolated from the injured lungs. Neutrophils were isolated from the mouse lungs at 24 h after LPS instillation. The isolated neutrophils were cultured in either media alone (RPMI 1640 supplemented with 10% FCS), media containing CXCL12, media containing CXCL12 and a specific CXCR4 antagonist or media with a specific CXCR4 antagonist alone for 24 h at 37 °C. Subsequently, cell death was assessed by trypan blue staining (**a**). Staining with Annexin V and 7-AAD was also performed to detect early apoptotic (Annexin $V^+7\text{-}AAD^-$; **b**, **c**) cells and late apoptotic/necrotic (Annexin $V^+7\text{-}AAD^+$; **b**, **d**) cells. Representative dot plots are shown. A total of six mice were used in each group. The values represent mean±s.e.m. $^*P<0.01$ versus before culture group and $^\dagger P<0.01$ versus media only group using ANOVA with Scheffé's *post hoc* test. 7-AAD, 7-aminoactinomycin D; FCS, fetal calf serum.

hematopoietic cells[32] and blood neutrophils of Warts, hypogammaglobulinemia, infections, and myelokathexis syndrome (an inherited immune disorder associated with CXCR4 gene mutation, causing a defect of CXCR4 internalization) patients[34] *via* ERK1/2 and/or PI3K/Akt signaling pathway. Western blotting revealed that CXCL12 induced phosphorylation of both ERK1/2 and Akt (Figure 5a) in the neutrophils isolated from the injured lungs. Moreover, the protective effect of CXCL12 against spontaneous apoptosis on the neutrophils was suppressed by the presence of MEK1/2 inhibitor or PI3K inhibitor (Figure 5b and c). These findings suggested the protective effect of CXCL12/CXCR4 against cell death of the neutrophils accumulated in the lungs during LPS-induced lung injury through ERK and PI3K/Akt signaling pathways.

L-selectin may be involved in the increase in surface CXCR4 expression on neutrophils

Our findings suggested that the increase in surface CXCR4 expression levels occurred during or after the extravasation of neutrophils in the lungs during LPS-induced lung injury. Circulating neutrophils expressed L-selectin on their surface (Figure 6a), whereas significant levels of surface L-selectin expression were not observed on neutrophils in lung digests and BAL fluids during LPS-induced lung injury (Figure 6b and c). These findings suggested that the shedding of L-selectin occurred in the process of extravasation of neutrophils into the injured lungs. To elucidate the participation of L-selectin in the increase in surface CXCR4 expression on neutrophils, we stimulated circulating neutrophils *ex vivo* with sulfatide, one of the native

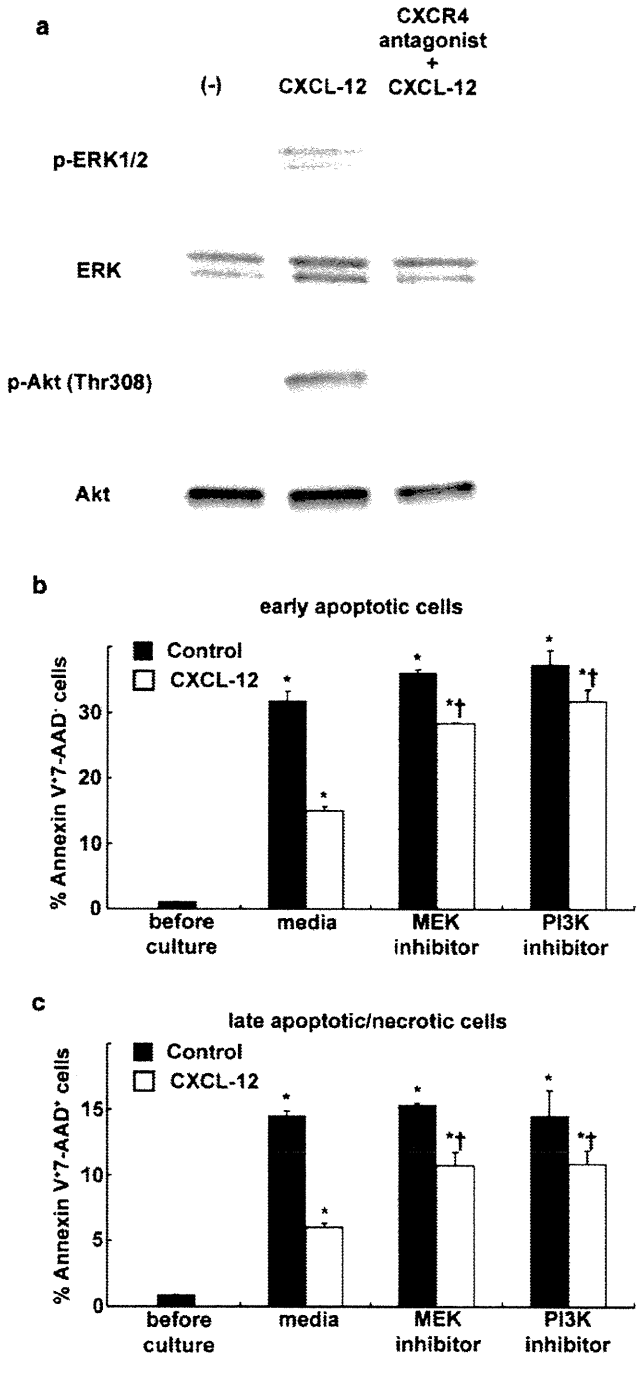

Figure 5 CXCL12 protects lung-accumulated neutrophils of LPS-injured mice from apoptosis through MEK/ERK and PI3K/Akt pathways. (**a**) Neutrophils were isolated from the mouse lungs at 24 h after LPS instillation. Isolated neutrophils were untreated or pre-incubated with a CXCR4 antagonist then treated CXCL12. Western blot analysis showed that CXCL12 induced the phosphorylation of ERK1/2 and Akt. (**b**, **c**) The isolated neutrophils were cultured for 24 h at 37 °C in the presence (white bar) or absence (black bar) of CXCL12 alone or in combination with a MEK1/2 inhibitor (U0126) or a PI3K inhibitor (LY294002). Subsequently, staining with Annexin V and 7-AAD was also performed to detect early apoptotic (Annexin V^+ 7-AAD$^-$; **b**) cells and late apoptotic/necrotic (Annexin V^+ 7-AAD^+; **c**) cells. Note the suppression of the inhibitory effect of CXCL12 against apoptosis in the presence of MEK1/2 inhibitor or PI3K inhibitor. The values represent mean±s.e.m. (n=6). *P<0.01 versus before culture group and $^{\dagger}P$<0.01 versus media only group using ANOVA with Scheffé's *post hoc* test. 7-AAD, 7-aminoactinomycin D; LPS, lipopolysaccharide.

L-selectin ligands,[35] and examined the changes in CXCR4 expression. Sulfatide induced a significant increase in surface CXCR4 expression on neutrophils (Figure 6d–f) and shedding of L-selectin (Figure 6g and h). This finding suggested that L-selectin may be involved in the increase in surface CXCR4 expression on neutrophils after the emigration of these cells into the injured lungs.

DISCUSSION

In the present study, we demonstrated that cell surface CXCR4 expression levels increase on extravascular neutrophils, but not on intravascular neutrophils, in the injured lung during LPS-induced lung injury. Because CXCL12 is also upregulated in the injured lungs,[17–19] these findings suggest that the increase in surface CXCR4 expression levels on extravasated neutrophils acts together with the increase of CXCL12 in the lungs to promote neutrophil migration and/or retention within the airspace.

To investigate whether the CXCL12/CXCR4 signaling system contributes to neutrophil migration to the lung or retention in the injured lung, we examined the migratory activities of neutrophils isolated from the bone marrow, blood, lung digests and BAL fluids of LPS-injured mice toward CXCL12. Our findings revealed that neutrophils isolated from lung digests and BAL fluids exhibited enhanced migratory activities toward CXCL12, whereas neutrophils isolated from bone marrow or blood did not. These findings were consistent with the low levels of surface CXCR4 expression found on neutrophils isolated from bone marrow and blood (Figure 1a and b). These data suggest that the neutrophils that were accumulated in the lung acquired the ability to migrate toward CXCL12 through the increase in CXCR4 and that the CXCL12/CXCR4 signaling pathway contributes primarily to neutrophil retention, not migration, in cases of LPS-induced lung injury.

We examined whether CXCR4 activation by CXCL12 prevented cell death of lung neutrophils, because the apoptosis of neutrophils and subsequent macrophage phagocytosis of apoptotic cells contribute to neutrophil clearance. We found that CXCL12 reduced the levels of cell death of the extravasated neutrophils within the injured lungs. This protective effect was inhibited when a specific CXCR4 antagonist was administered. We investigated the mechanisms for how CXCL12/CXCR4 signaling protects the lung accumulated neutrophils and then revealed that CXCL12 protects the neutrophils from apoptosis through MEK/ERK and PI3K/Akt pathways. Although we do not have clear evidence confirming that CXCR4 activation is critical for the survival of accumulated neutrophils *in vivo*, this idea is compatible with a recent clinical report describing increased CXCL12 concentrations and the presence of primarily non-apoptotic neutrophils with enhanced CXCR4 expression levels in the BAL fluid of lipopolysaccharide patients.[36] Taken together, our *ex vivo* findings suggest that this protective effect of the CXCL12/CXCR4 signaling pathway against cell death contributes to neutrophil accumulation and retention in the lungs during inflammatory diseases, including cases of acute lung injury.

To investigate the stimuli that induce the increase in surface CXCR4 expression on neutrophils, we focused on L-selectin, a cell adhesion molecule that belongs to the selectin family, because it has been also reported that L-selectin is involved in the increase in surface CXCR4 expression on human peripheral blood lymphocytes and mouse

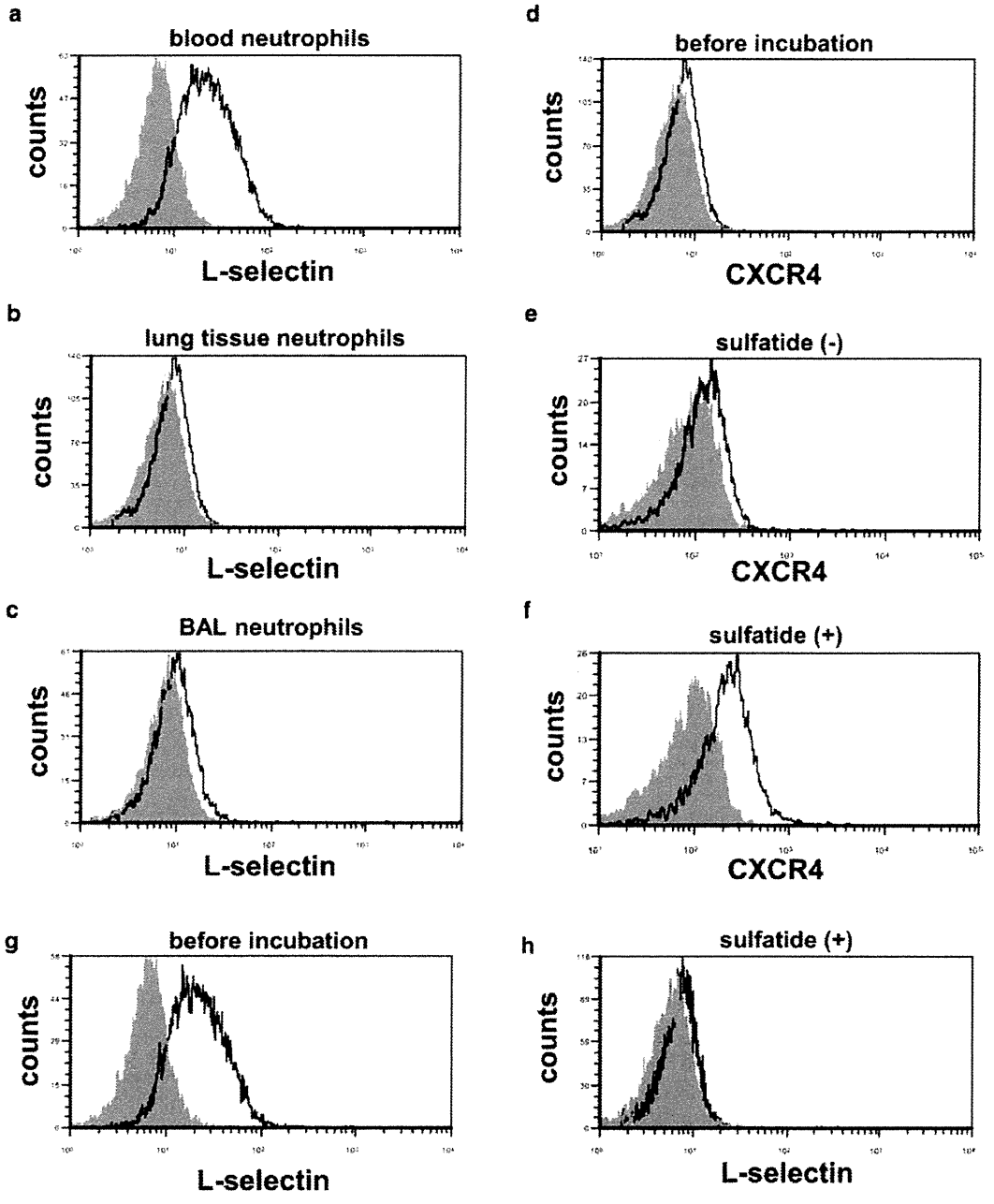

Figure 6 L-selectin may be involved in the increase in surface CXCR4 expression in mouse neutrophils. (**a–c**) The surface L-selectin expression levels of neutrophils isolated from blood (**a**), lung tissue (**b**) and BAL fluid (**c**) at 24 h during LPS-induced lung injury were assessed by flow cytometry. The filled images show the staining using an isotype-matched control antibody. (**d–f**) Sulfatide induced the increase in surface CXCR4 expression in neutrophils isolated from mouse blood. The surface CXCR4 expression levels were examined before incubation (**d**) and after incubation for 1 h either with (**f**) or without (**e**) sulfatide. (**g, h**) Sulfatide induced shedding of L-selectin on neutrophils. Surface expressions of L-selectin on neutrophils were examined before incubation (**g**) and after incubation for 1 h with sulfatide (**h**). Representative histograms from one of three experiments that showed similar results are presented. BAL, bronchoalveolar lavage; LPS, lipopolysaccharide.

lymphocytes.[20,21] We observed that the shedding of L-selectin, which is induced by L-selectin activation, occurred during the process of extravasation of neutrophils (Figure 6a–c). We also found that sulfatide, a natural ligand for L-selectin, induced the surface expression of CXCR4 on neutrophils isolated from mouse blood. These findings suggest that the activation of L-selectin may be involved in the increase in surface CXCR4 expression levels on neutrophils in the lungs.

In summary, we have shown that the surface CXCR4 expression levels on neutrophils increase after extravasation into the mouse lungs during LPS-induced lung injury. In addition, the activation of L-selectin may be a key regulator of this surface CXCR4 increase. Our findings suggest that the CXCL12/CXCR4 signaling pathway is involved in neutrophil accumulation and retention in the inflammatory site through both its chemotactic effect and its protective effect against cell death.

Supplementary information accompanies the paper on Cellular & Molecular Immunology's website (http://www.nature.com/cmi/)

ACKNOWLEDGEMENTS

This work was supported by grants from the Japanese Society for the Promotion of Science (no. 17590776 to HK and no. 17790524 to MY). The authors declare no financial or commercial conflict of interest.

1 Kubo H, Graham L, Doyle NA, Quinlan WM, Hogg JC, Doerschuk CM. Complement fragment-induced release of neutrophils from bone marrow and sequestration within pulmonary capillaries in rabbits. *Blood* 1998; **92**: 283–290.
2 Kubo H, Morgenstern D, Quinian WM, Ward PA, Dinauer MC, Doerschuk CM. Preservation of complement-induced lung injury in mice with deficiency of NADPH oxidase. *J Clin Invest* 1996; **97**: 2680–2684.
3 Strieter RM, Kunkel SL, Bone RC. Role of tumor necrosis factor-alpha in disease states and inflammation. *Crit Care Med* 1993; **21**: S447–S463.
4 Gabay C, Lamacchia C, Palmer G. IL-1 pathways in inflammation and human diseases. *Nat Rev Rheumatol* 2010; **6**: 232–241.
5 Romagnani P, Lasagni L, Annunziato F, Serio M, Romagnani S. CXC chemokines: the regulatory link between inflammation and angiogenesis. *Trends Immunol* 2004; **25**: 201–209.
6 Harada A, Sekido N, Akahoshi T, Wada T, Mukaida N, Matsushima K. Essential involvement of interleukin-8 (IL-8) in acute inflammation. *J Leukoc Biol* 1994; **56**: 559–564.
7 Zachariae CO. Chemotactic cytokines and inflammation. Biological properties of the lymphocyte and monocyte chemotactic factors ELCF, MCAF and IL-8. *Acta Derm Venereol Suppl (Stockh)* 1993; **181**: 1–37.
8 Bleul CC, Farzan M, Choe H, Parolin C, Clark-Lewis I, Sodroski J *et al.* The lymphocyte chemoattractant SDF-1 is a ligand for LESTR/fusin and blocks HIV-1 entry. *Nature* 1996; **382**: 829–833.
9 Bleul CC, Fuhlbrigge RC, Casasnovas JM, Aiuti A, Springer TA. A highly efficacious lymphocyte chemoattractant, stromal cell-derived factor 1 (SDF-1). *J Exp Med* 1996; **184**: 1101–1109.
10 Nagasawa T, Nakajima T, Tachibana K, Iizasa H, Bleul CC, Yoshie O *et al.* Molecular cloning and characterization of a murine pre-B-cell growth-stimulating factor/stromal cell-derived factor 1 receptor, a murine homolog of the human immunodeficiency virus 1 entry coreceptor fusin. *Proc Natl Acad Sci USA* 1996; **93**: 14726–14729.
11 Oberlin E, Amara A, Bachelerie F, Bessia C, Virelizier JL, Arenzana-Seisdedos F *et al.* The CXC chemokine SDF-1 is the ligand for LESTR/fusin and prevents infection by T-cell-line-adapted HIV-1. *Nature* 1996; **382**: 833–835.
12 Liles WC, Broxmeyer HE, Rodger E, Wood B, Hubel K, Cooper S *et al.* Mobilization of hematopoietic progenitor cells in healthy volunteers by AMD3100, a CXCR4 antagonist. *Blood* 2003; **102**: 2728–2730.
13 Broxmeyer HE, Orschell CM, Clapp DW, Hangoc G, Cooper S, Plett PA *et al.* Rapid mobilization of murine and human hematopoietic stem and progenitor cells with AMD3100, a CXCR4 antagonist. *J Exp Med* 2005; **201**: 1307–1318.
14 Eash KJ, Means JM, White DW, Link DC. CXCR4 is a key regulator of neutrophil release from the bone marrow under basal and stress granulopoiesis conditions. *Blood* 2009; **113**: 4711–4719.
15 Suratt BT, Petty JM, Young SK, Malcolm KC, Lieber JG, Nick JA *et al.* Role of the CXCR4/SDF-1 chemokine axis in circulating neutrophil homeostasis. *Blood* 2004; **104**: 565–571.
16 Martin C, Burdon PC, Bridger G, Gutierrez-Ramos JC, Williams TJ, Rankin SM. Chemokines acting *via* CXCR2 and CXCR4 control the release of neutrophils from the bone marrow and their return following senescence. *Immunity* 2003; **19**: 583–593.
17 Petty JM, Sueblinvong V, Lenox CC, Jones CC, Cosgrove GP, Cool CD *et al.* Pulmonary stromal-derived factor-1 expression and effect on neutrophil recruitment during acute lung injury. *J Immunol* 2007; **178**: 8148–8157.
18 Yamada M, Kubo H, Kobayashi S, Ishizawa K, Sasaki H. Stromal cell-derived factor-1 contributes to lipopolysaccharide-induced lung injury. *Am J Respir Crit Care Med* 2004; **169**: A875.
19 Yamada M, Kubo H, Kobayashi S, Ishizawa K, Sasaki H. Stromal cell-derived factor-1 contributes to lipopolysaccharide-induced neutrophil emigration within the airspace. *Proc Am Thorac Soc* 2005; **2**: A350.
20 Duchesneau P, Gallagher E, Walcheck B, Waddell TK. Up-regulation of leukocyte CXCR4 expression by sulfatide: an L-selectin-dependent pathway on $CD4^+$ T cells. *Eur J Immunol* 2007; **37**: 2949–2960.
21 Ding Z, Issekutz TB, Downey GP, Waddell TK. L-selectin stimulation enhances functional expression of surface CXCR4 in lymphocytes: implications for cellular activation during adhesion and migration. *Blood* 2003; **101**: 4245–4252.
22 Palecanda A, Walcheck B, Bishop DK, Jutila MA. Rapid activation-independent shedding of leukocyte L-selectin induced by cross-linking of the surface antigen. *Eur J Immunol* 1992; **22**: 1279–1286.
23 Kishimoto TK, Jutila MA, Berg EL, Butcher EC. Neutrophil Mac-1 and MEL-14 adhesion proteins inversely regulated by chemotactic factors. *Science* 1989; **245**: 1238–1241.
24 Jutila MA, Berg EL, Kishimoto TK, Picker LJ, Bargatze RF, Bishop DK *et al.* Inflammation-induced endothelial cell adhesion to lymphocytes, neutrophils, and monocytes. Role of homing receptors and other adhesion molecules. *Transplantation* 1989; **48**: 727–731.
25 Fujii N, Nakashima H, Tamamura H. The therapeutic potential of CXCR4 antagonists in the treatment of HIV. *Expert Opin Investig Drugs* 2003; **12**: 185–195.
26 Tamamura H, Hiramatsu K, Mizumoto M, Ueda S, Kusano S, Terakubo S *et al.* Enhancement of the T140-based pharmacophores leads to the development of more potent and bio-stable CXCR4 antagonists. *Org Biomol Chem* 2003; **1**: 3663–3669.
27 Reutershan J, Basit A, Galkina EV, Ley K. Sequential recruitment of neutrophils into lung and bronchoalveolar lavage fluid in LPS-induced acute lung injury. *Am J Physiol Lung Cell Mol Physiol* 2005; **289**: L807–L815.
28 Tamamura H, Fujisawa M, Hiramatsu K, Mizumoto M, Nakashima H, Yamamoto N *et al.* Identification of a CXCR4 antagonist, a T140 analog, as an anti-rheumatoid arthritis agent. *FEBS Lett* 2004; **569**: 99–104.
29 Matute-Bello G, Winn RK, Jonas M, Chi EY, Martin TR, Liles WC. Fas (CD95) induces alveolar epithelial cell apoptosis *in vivo* implications for acute pulmonary inflammation. *Am J Pathol* 2001; **158**: 153–161.
30 Hendrix CW, Flexner C, MacFarland RT, Giandomenico C, Fuchs EJ, Redpath E *et al.* Pharmacokinetics and safety of AMD-3100, a novel antagonist of the CXCR-4 chemokine receptor, in human volunteers. *Antimicrob Agents Chemother* 2000; **44**: 1667–1673.
31 Hubel K, Liles WC, Broxmeyer HE, Rodger E, Wood B, Cooper S *et al.* Leukocytosis and mobilization of $CD34^+$ hematopoietic progenitor cells by AMD3100, a CXCR4 antagonist. *Support Cancer Ther* 2004; **1**: 165–172.
32 Lataillade JJ, Clay D, Bourin P, Herodin F, Dupuy C, Jasmin C *et al.* Stromal cell-derived factor 1 regulates primitive hematopoiesis by suppressing apoptosis and by promoting G_0/G_1 transition in $CD34^+$ cells: evidence for an autocrine/paracrine mechanism. *Blood* 2002; **99**: 1117–1129.
33 Vlahakis SR, Villasis-Keever A, Gomez T, Vanegas M, Vlahakis N, Paya CV. G protein-coupled chemokine receptors induce both survival and apoptotic signaling pathways. *J Immunol* 2002; **169**: 5546–5554.
34 Sanmun D, Garwicz D, Smith CI, Palmblad J, Fadeel B. Stromal-derived factor-1 abolishes constitutive apoptosis of WHIM syndrome neutrophils harbouring a truncating CXCR4 mutation. *Br J Haematol* 2006; **134**: 640–644.
35 Suzuki Y, Toda Y, Tamatani T, Watanabe T, Suzuki T, Nakao T *et al.* Sulfated glycolipids are ligands for a lymphocyte homing receptor, L-selectin (LECAM-1), binding epitope in sulfated sugar chain. *Biochem Biophys Res Commun* 1993; **190**: 426–434.
36 Hartl D, Krauss-Etschmann S, Koller B, Hordijk PL, Kuijpers TW, Hoffmann F *et al.* Infiltrated neutrophils acquire novel chemokine receptor expression and chemokine responsiveness in chronic inflammatory lung diseases. *J Immunol* 2008; **181**: 8053–8067.

Cutting Edge

THE JOURNAL OF IMMUNOLOGY

Cutting Edge: T Cells Monitor N-Myristoylation of the Nef Protein in Simian Immunodeficiency Virus-Infected Monkeys

Daisuke Morita,*,† Tatsuhiko Igarashi,‡ Mariko Horiike,‡ Naoki Mori,§ and Masahiko Sugita*,†

The use of the host cellular machinery is essential for pathogenic viruses to replicate in host cells. HIV and SIV borrow the host-derived N-myristoyl-transferase and its substrate, myristoyl-CoA, for coupling a saturated C_{14} fatty acid (myristic acid) to the N-terminal glycine residue of the Nef protein. This biochemical reaction, referred to as N-myristoylation, assists its targeting to the plasma membrane, thereby supporting the immunosuppressive activity proposed for the Nef protein. In this study, we show that the host immunity is equipped with CTLs capable of sensing N-myristoylation of the Nef protein. A rhesus macaque $CD8^+$ T cell line was established that specifically recognized N-myristoylated, but not unmodified, peptides of the Nef protein. Furthermore, the population size of N-myristoylated Nef peptide-specific T cells was found to increase significantly in the circulation of SIV-infected monkeys. Thus, these results identify N-myristoylated viral peptides as a novel class of CTL target Ag. ***The Journal of Immunology,*** **2011, 187: 608–612.**

Major histocompatability complex class I-restricted CTLs are a critical component of the host immunity, capable of detecting virus-infected cells and eliminating them to clear infection. However, pathogenic viruses often exhibit an outstanding ability to escape from CTL attack by introducing amino acid mutations in the target proteins while maintaining their proper functions. Therefore, CTL recognition of antigenic epitopes that admit of no arbitrary mutations would be crucial for efficient host defense and CTL-based vaccine development.

Recently, the repertoire of Ags recognized by T cells has been expanded to include not only proteins but also lipidic molecules. For example, it has been demonstrated that human CD1b-restricted T cells can recognize mycobacteria-derived mycolic acids and their glycosylated species, which are critical components for the cell wall architecture of mycobacteria (1). It remains to be established whether T cell responses to these lipidic Ags could significantly contribute to host defense against human tuberculosis, but their protective role has been noted in the guinea pig model of tuberculosis (2).

Viruses do not possess their own lipids, but can biosynthesize lipopeptides by using the host cellular machinery. Given that N-myristoylation is an irreversible protein modification that occurs in the conserved motifs spanning the N-terminal short stretch of several amino acid residues (3) and that N-myristoylation of the Nef protein is critical for HIV pathogenesis (4), we reasoned that N-myristoylated Nef peptides would be an ideal Ag targeted by the host CTL response. In this study, we successfully established a rhesus macaque $CD8^+$ T cell line that specifically recognized N-myristoylated peptides of the SIV Nef protein. More importantly, these N-myristoylated Nef peptide-specific T cells were found to expand significantly in SIV-infected monkeys.

Materials and Methods

Ags

Chemical reagents were purchased from Nacalai Tesque (Kyoto, Japan) unless otherwise indicated. Peptides were synthesized by a manual Fmoc solid-phase peptide synthesis technique using Wang-resin precoupled with a relevant C-terminal amino acid (EMD Chemicals, Gibbstown, NJ). Acylation was carried out by reacting the N-terminal amino group with acid anhydrides prepared with *N,N'*-diisopropylcarbodiimide, followed by release of the acylated peptides in 95% trifluoroacetic acid. Crude Ags were purified by HPLC with a gradient elution based on water and methanol with 0.1% trifluoroacetic acid. After freeze-drying, the samples were subjected to liquid chromatography mass spectrometry analysis, using a C18 column (GL Sciences) at a flow rate of 0.5 ml/min with a solvent system of water and methanol with 0.1% formic acid.

Establishment of lipopeptide-specific T cell lines

PBMCs (1.2×10^7/well) obtained from rhesus macaque monkeys were cultured with synthetic lipopeptides at a concentration of 5 μg/ml, and antigenic stimulation was repeated every 2 wk in the presence of irradiated autologous PBMCs. IL-2 was added at 0.3 nM after the second stimulation, and the concentration was gradually increased to 3 nM by the fourth stimulation. The culture medium used was RPMI 1640 (Invitrogen, Carlsbad,

*Laboratory of Cell Regulation, Institute for Virus Research, Kyoto University, Kyoto 606-8507, Japan; †Laboratory of Cell Regulation and Molecular Network, Graduate School of Biostudies, Kyoto University, Kyoto 606-8501, Japan; ‡Laboratory of Primate Model, Institute for Virus Research, Kyoto University, Kyoto 606-8507, Japan; and §Division of Applied Life Sciences, Graduate School of Agriculture, Kyoto University, Kyoto 606-8502, Japan

Received for publication April 26, 2011. Accepted for publication May 19, 2011.

This work was supported by grants from the Ministry of Education, Culture, Sports, Science and Technology and from the Japan Society for the Promotion of Science (to M.S.).

Address correspondence and reprint requests to Prof. Masahiko Sugita or Prof. Tatsuhiko Igarashi, Laboratory of Cell Regulation, Institute for Virus Research, Kyoto University, 53 Kawahara-cho, Shogoin, Sakyo-ku, Kyoto, Japan (M.S.) or Laboratory of Primate Model, Institute for Virus Research, Kyoto University, 53 Kawahara-cho, Shogoin, Sakyo-ku, Kyoto, Japan (T.I.). E-mail addresses: msugita@virus.kyoto-u.ac.jp (M.S.) and tigarash@virus.kyoto-u.ac.jp (T.I.)

Abbreviation used in this article: PI, propidium iodide.

www.jimmunol.org/cgi/doi/10.4049/jimmunol.1101216

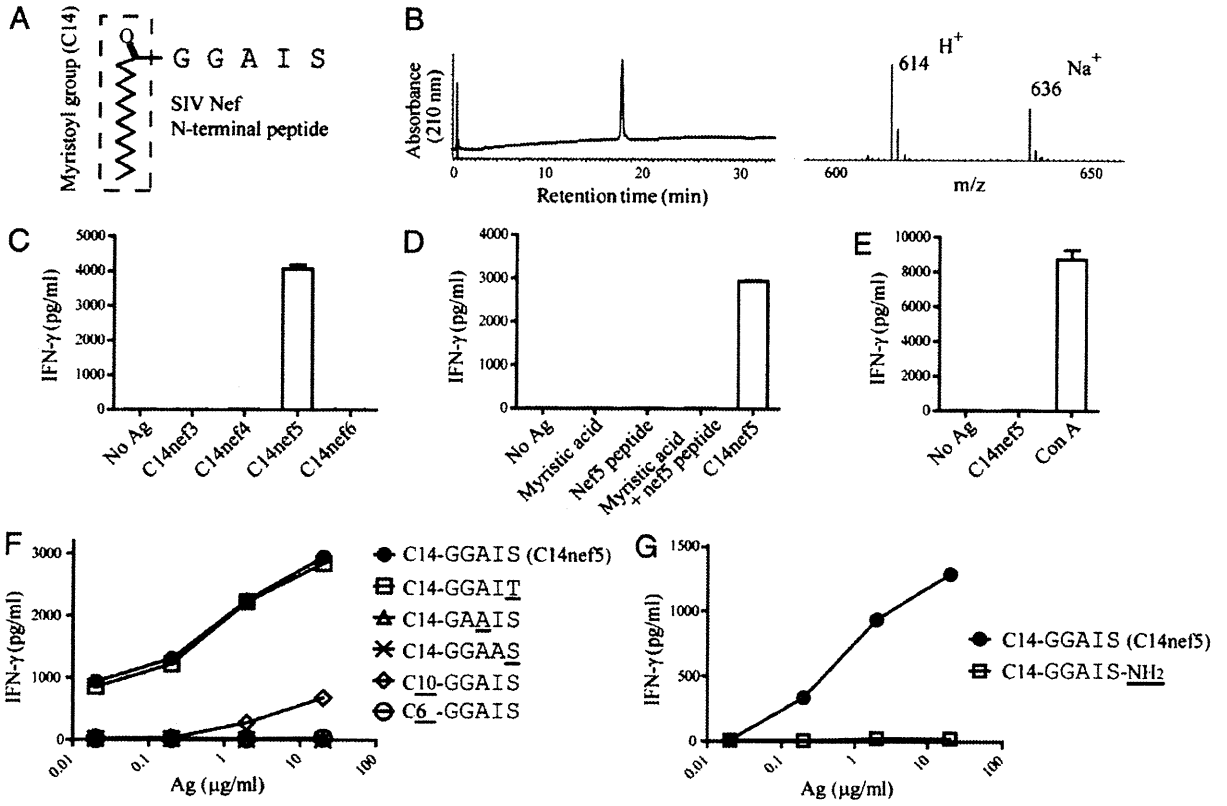

FIGURE 1. The response of 2N5.1 to N-myristoylated Nef peptides. *A*, The N-terminal 5-mer peptide derived from the mac239 strain of SIV was synthesized, and a myristic acid was conjugated with the glycine residue to generate the C14nef5 lipopeptide. *B*, The synthetic compound was analyzed by liquid chromatography mass spectrometry. A single peak was observed at a retention time of 19 min (*left panel*), and the ions with a mass-to-charge ratio of 614.4 and 636.4 were detected that corresponded to the proton and sodium adducts of C14nef5 with the exact mass of 613.41 (*right panel*). *C* and *D*, The 2N5.1 T cells (5×10^4/well) were stimulated with the indicated Ags (5 μg/ml) in the presence of irradiated autologous PBMCs (3×10^5), and the amount of IFN-γ released into the culture media was measured. Assays were performed in triplicate samples, and the mean values with the SD are shown. *E*, PBMCs (3×10^5/well) were incubated with medium, C14nef5, or Con A (5 μg/ml), and the amount of secreted IFN-γ was measured. *F* and *G*, The 2N5.1 T cells were stimulated with either C14nef5 or mutant Ags, and the amount of IFN-γ released into the media was measured.

CA) supplemented with 10% heat-inactivated FCS (Hyclone, Logan, UT), 2-ME (Invitrogen), penicillin, and streptomycin.

T cell assays

T cells (5×10^4/well) were incubated with the indicated concentrations of Ags in the presence of irradiated autologous or allogeneic PBMCs (3×10^5/well) using 96-well, flat-bottom microtiter plates. After 24 h, aliquots of the culture supernatants were collected, and the amount of IFN-γ released into the media was measured using a human/monkey IFN-γ ELISA kit (Mabtech, Nacka Strand, Sweden).

Flow cytometry

The surface expression of T cell markers on the 2N5.1 T cells was analyzed by flow cytometry as described previously (5). For the cytotoxicity assay, the T cell line was labeled by incubating the cells with 500 nM CFSE (Invitrogen) for 10 min at 37°C. Allogeneic PBMCs (3×10^5/well) were cultured in the presence or absence of the CSFE-labeled 2N5.1 T cells (1×10^5/well) and/or the C14nef5 Ag (5 μg/ml). After 4.5 h culture, the whole cells were harvested and stained with PE-labeled mouse mAbs to CD3 (SP34-2), CD14 (M5E2), or CD20 (2H7) for 30 min on ice. The labeled cells were washed, and propidium iodide (PI; BD Biosciences) was added to gate out dead cells. The cell samples were analyzed by flow cytometry using a BD FACSCanto II flow cytometer (BD Biosciences). Data were collected at a constant flow rate (120 μl/min).

Animals and viral infection

The rhesus macaques (*Macaca mulatta*) used in this study were treated humanely in accordance with the institutional regulations, and experimental protocols were approved by the Committee for Experimental Use of Non-human Primates at the Institute for Virus Research, Kyoto University. Six healthy monkeys were inoculated with SIVmac239 (6) i.v. at a dose of 2000 50% tissue culture-infective dose, and the titer of plasma viral RNA was determined by quantitative RT-PCR as described previously (7).

IFN-γ ELISPOT assays

ELISPOT plates (Millipore, Billerica, MA) were coated with the GZ-4 anti–IFN-γ Ab (10 μg/ml) at 4°C overnight. After blocking with RPMI 1640

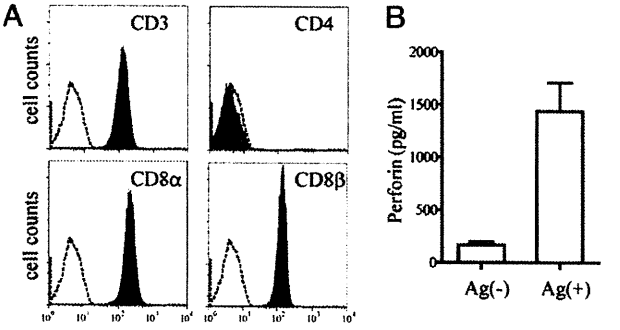

FIGURE 2. Expression of CD8 molecules and perforin by the 2N5.1 T cells. *A*, The 2N5.1 T cells were tested for their expression of T cell markers by flow cytometry. A dotted line in each panel indicates a histogram with a negative control Ab. *B*, The 2N5.1 T cells (5×10^4/well) were cultured with autologous PBMCs (3×10^5/well) in either the presence or the absence of the C14nef5 Ag (5 μg/ml), and the amount of perforin released into the culture media was measured.

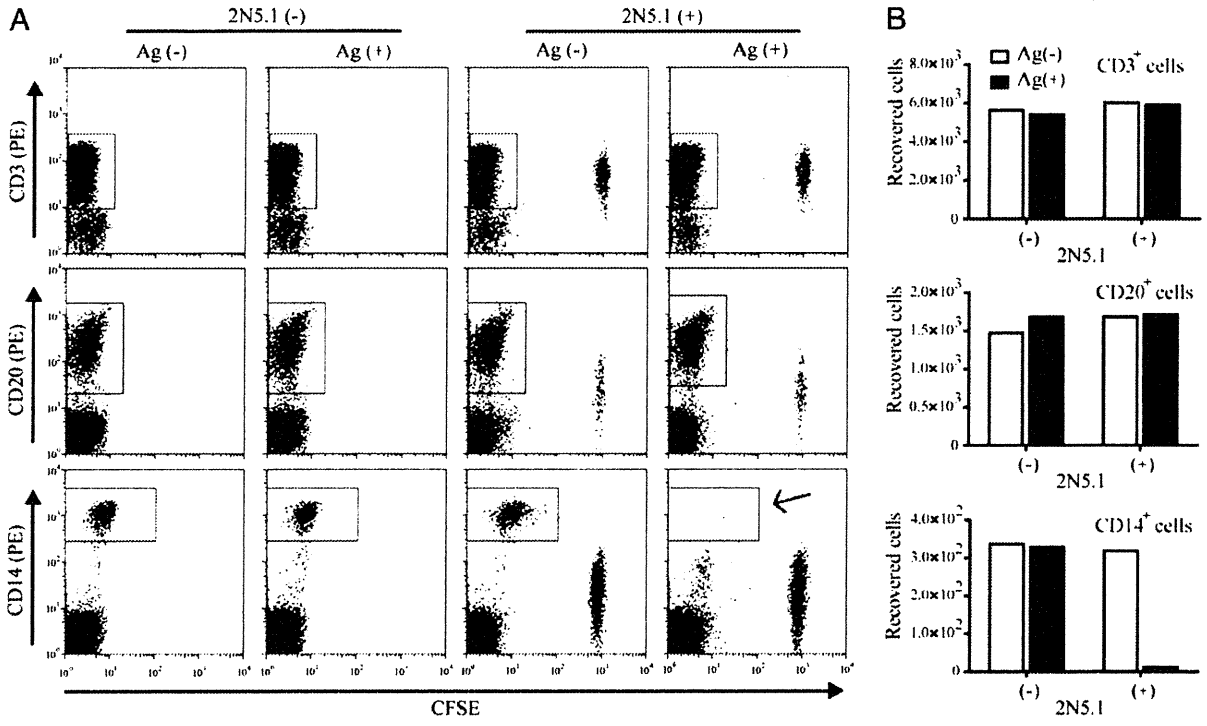

FIGURE 3. Elimination of C14nef5-pulsed monocytes by the 2N5.1 T cells. *A*, Allogeneic PBMCs (3×10^5/well) were incubated in either the presence or the absence of the CFSE-labeled 2N5.1 T cells (1×10^5/well) and the C14nef5 Ag for 4.5 h. The cells were then stained with PE-labeled Abs to CD3, CD20, or CD14, and PI-unstained live cells were analyzed by flow cytometry. PBMC-derived T cells, B cells, and monocytes that survived were boxed in the *top, middle,* and *bottom panels,* respectively. Note that monocytes were specifically eliminated when PBMCs were incubated in the presence of the 2N5.1 T cells and the C14nef5 Ag (indicated with an arrow). *B*, The absolute number of recovered $CD3^+$ (*top panel*), $CD20^+$ (*middle panel*), and $CD14^+$ cells (*bottom panel*) during 1 min of flow cytometric analysis is shown.

supplemented with 10% FCS, monkey PBMCs (2.5×10^5/well) were incubated with Ags (5 μg/ml) for 20 h. The plates were then washed with PBS, and spots representing IFN-γ–secreting cells were detected by sequential incubation with the biotinylated 7-B6-1 anti–IFN-γ Ab (1 μg/ml) for 2 h at room temperature, followed by HRP-conjugated streptavidin for 1 h and tetramethylbenzidine for 10 min (all from Mabtech). Samples were analyzed in duplicate, and the mean numbers of the spots were calculated.

Results and Discussion

To address whether T cells could specifically recognize N-myristoylated Nef peptides, PBMCs obtained from rhesus macaque (*M. mulatta*) monkeys were stimulated repeatedly in an in vitro culture with an array of synthetic N-myristoylated peptides derived from the SIV Nef protein. As a result of this attempt, a T cell line, termed 2N5.1, was established that proliferated in response to the N-myristoylated Nef 5-mer peptide (C14nef5) (Fig. 1*A*, 1*B*). The cells produced IFN-γ in response to C14nef5, but not N-myristoylated 3-mer (C14nef3), 4-mer (C14nef4), and 6-mer (C14nef6) of the Nef peptide (Fig. 1*C*). Furthermore, the 2N5.1 T cell activation was not observed when myristic acid and the 5-mer peptide were added as a free form (Fig. 1*D*), suggesting that

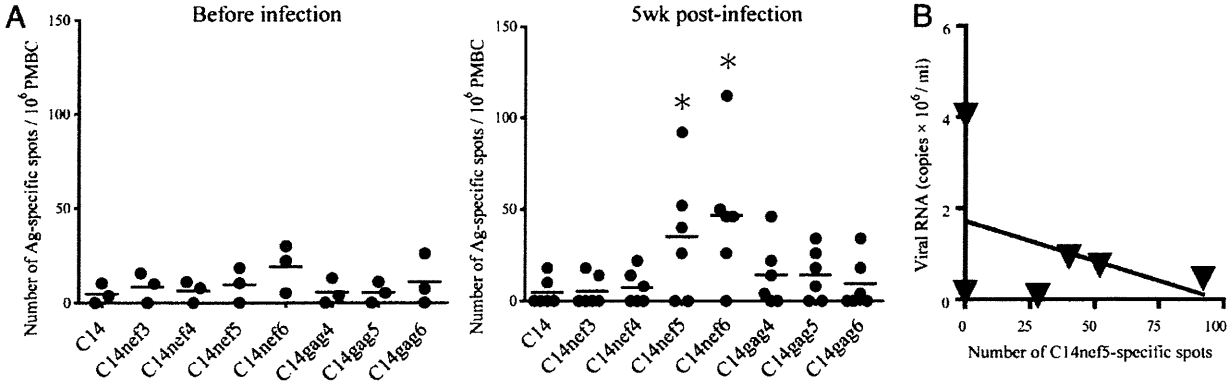

FIGURE 4. T cell responses to myristoylated Nef peptides in SIV-infected monkeys. *A*, Six healthy rhesus monkeys were inoculated with SIVmac239 i.v. at a dose of 2000 50% tissue culture-infective dose. Before ($n = 3$, *left panel*) and 5 wk postinfection ($n = 6$, *right panel*), PBMCs were obtained and stimulated with the indicated Ags, followed by detection of IFN-γ–producing cells in ELISPOT assays. The numbers of Ag-specific spots in individual subjects are shown with dots, and the mean values are indicated with bars. *B*, The numbers of C14nef5-specific spots and the virus load at 7 wk postinfection are plotted for each subject. The linear line was drawn on the basis of the linear least-square method, and the value of correlation coefficient was −0.41 ($n = 6$). *$p < 0.05$.

the T cells specifically recognized the 5-mer peptide that was conjugated covalently with myristic acid. Freshly isolated PBMCs responded to Con A, but not C14nef5 (Fig. 1*E*), ruling out the possibility that C14nef5 functioned as a non-specific T cell mitogen.

An additional series of mutational analyses revealed a fine specificity for the lipopeptide recognition by the T cells. The 5-mer Nef peptide conjugated with a shorter (C_{10}) saturated fatty acid (C10-GGAIS) showed reduced T cell stimulation activity compared with C14nef5, and no T cell response was detected for C6-GGAIS (Fig. 1*F*), further confirming that the peptide modification with a fatty acid of the C_{14} chain length (myristic acid) was essential for activation of the 2N5.1 cells. The N-terminal amino acid sequence (GGAIS) of the Nef protein matches with a typical N-myristoylation motif, Gly-X-X-X-(Ser/Thr), in which X is any amino acid (3). Whereas the serine-to-threonine substitution (C14-GGAIT) did not affect the antigenic activity, alanine substitution for either the second glycine residue (C14-GAAIS) or the isoleucine residue (C14-GGAAS) located between the conserved flanking amino acid residues totally abrogated the activity (Fig. 1*F*). Furthermore, addition of an amide linkage to the carboxyl group of the C-terminal serine residue (C14-GGAIS-NH_2) resulted in total loss of the antigenic activity (Fig. 1*G*). These results indicated that the amino acid sequence of the C14nef5 lipopeptide constituted a T cell epitope that was short in length but still stringent in terms of amino acid selection compared with that recognized by classical MHC-restricted, peptide-specific T cells.

As expected from the highly specific recognition of peptide sequences, the 2N5.1 T cell line expressed clonotypic TCR α- and β-chains with random N-additions (data not shown). The 2N5.1 T cells were found to be CD4 negative and positive for CD8α- and CD8β-chains (Fig. 2*A*). Upon antigenic stimulation, the cells could secrete perforin (Fig. 2*B*), suggesting that the 2N5.1 T cells were both phenotypically and functionally defined as CTLs. To directly assess the Ag-dependent cytolytic activity exerted by the T cells, freshly isolated PBMCs were used as target cells for CFSE-labeled 2N5.1 T cells in an in vitro culture in either the presence or absence of the C14nef5 Ag. After 4.5 h, all of the cells were harvested and labeled with PE-conjugated Abs to CD3, CD20, or CD14. Whereas PI-stained dead cells were gated out, PBMC-derived T cells ($CD3^+$, $CSFE^-$ cells), B cells ($CD20^+$ cells), and monocytes ($CD14^+$ cells) as well as the 2N5.1 effector cells ($CSFE^+$ cells) were monitored by flow cytometry (Fig. 3*A*). The cell populations representing the recovered target T cells (Fig. 3*A*, boxed in the *top panels*) and B cells (Fig. 3*A*, boxed in the *middle panels*) were unchanged throughout the panels, and the absolute numbers of the cells were virtually the same regardless of the presence or absence of the T cells and the C14nef5 Ag (Fig. 3*B*, *top* and *middle panels*). In sharp contrast, the number of recovered $CD14^+$ monocytes was markedly reduced after culture in the presence of both the 2N5.1 T cells and the C14nef5 Ag (indicated with an arrow in Fig. 3*A* and shown in the *bottom panel* of Fig. 3*B*), demonstrating Ag-dependent killing of monocytes by the T cells. Consistent with this, peripheral blood monocytes purified by an MACS-based procedure could fully stimulate the 2N5.1 cells to produce IFN-γ (data not shown). On the basis of these observations, we concluded that the C14nef5-specific T cells were CTLs with monocytes as a major target cell type.

The results described above underscored the capacity for T cells to recognize the myristoylated Nef peptide, but the relevance of this to SIV infection in vivo remained to be established. We therefore wished to determine if such T cell responses directed specifically against myristoylated viral peptides might be elicited in SIV-infected monkeys. PBMCs were obtained from monkeys before and 5 wk postinfection with the mac239 strain of SIV and tested for their reactivity to C14nef3, C14nef4, C14nef5, C14nef6, and three N-terminally myristoylated SIV Gag peptides, C14-GVRN (C14gag4), C14-GVRNS (C14gag5), and C14-GVRNSV (C14gag6), in IFN-γ ELISPOT assays. Whereas no Ag-specific T cell responses were detected before infection, the number of T cells that recognized C14nef5 was significantly increased after SIV infection (Fig. 4*A*), suggesting that the immune recognition of C14nef5 indeed occurred in response to SIV infection. In addition, a significant fraction of T cells recognized C14nef6 in infected monkeys, which had not been expected from the study with the 2N5.1 T cell line. Finally, the plasma viral load at 7 wk postinfection in each SIV-infected monkey appeared to correlate reciprocally with the number of C14nef5-specific T cells (Fig. 4*B*).

It has been a challenge over the past two decades to develop effective vaccines against human infection with HIV. Unfortunately, the development of HIV vaccines designed for activating classical peptide-specific, MHC class I-restricted CTLs has had only limited success so far (8). The vaccine potential of the myristoylated Nef peptides will be tested directly, but one can predict that this new class of lipopeptide vaccine candidates may have a couple of important advantages over classical protein/peptide vaccines. Introducing amino acid mutations in the target proteins is an efficient strategy that HIV has evolved to escape from CTL attack, but the short stretch of the N-terminal amino acid residues of the Nef protein that contains N-myristoylation signal is hard to mutate without affecting the function of the protein (4). Although our preliminary studies indicated that the lipopeptide presentation could occur independently of CD1 function, the C14nef5-specific 2N5.1 T cell response was elicited by using PBMCs from any donor rhesus macaque monkeys as APCs, suggesting that the response could potentially be mediated by nonpolymorphic elements shared in all of the individuals. HIV uses the host cellular machinery for N-myristoylation of the Nef protein to favor its replication in the host, but the current study indicates that this results in unintended expansion of the Ag repertoire recognized by the host immune system. Lipid modifications are critical for a significant number of pathogenic viral proteins to function, but the host immunity appears to have evolved the ability to sense this post-translational event.

Acknowledgments

We thank Drs. Tomoyuki Miura and Isamu Matsunaga for helpful discussions.

Disclosures

The authors have no financial conflicts of interest.

References

1. Beckman, E. M., S. A. Porcelli, C. T. Morita, S. M. Behar, S. T. Furlong, and M. B. Brenner. 1994. Recognition of a lipid antigen by CD1-restricted alpha beta+ T cells. *Nature* 372: 691–694.
2. Dascher, C. C., K. Hiromatsu, X. Xiong, C. Morehouse, G. Watts, G. Liu, D. N. McMurray, K. P. LeClair, S. A. Porcelli, and M. B. Brenner. 2003. Immunization with a mycobacterial lipid vaccine improves pulmonary pathology in the guinea pig model of tuberculosis. *Int. Immunol.* 15: 915–925.
3. Boutin, J. A. 1997. Myristoylation. *Cell. Signal.* 9: 15–35.
4. Aldrovandi, G. M., L. Gao, G. Bristol, and J. A. Zack. 1998. Regions of human immunodeficiency virus type 1 nef required for function in vivo. *J. Virol.* 72: 7032–7039.
5. Morita, D., K. Katoh, T. Harada, Y. Nakagawa, I. Matsunaga, T. Miura, A. Adachi, T. Igarashi, and M. Sugita. 2008. Trans-species activation of human T cells by rhesus macaque CD1b molecules. *Biochem. Biophys. Res. Commun.* 377: 889–893.
6. Kestler, H. W., III, Y. Li, Y. M. Naidu, C. V. Butler, M. F. Ochs, G. Jaenel, N. W. King, M. D. Daniel, and R. C. Desrosiers. 1988. Comparison of simian immunodeficiency virus isolates. *Nature* 331: 619–622.
7. Igarashi, T., R. Iyengar, R. A. Byrum, A. Buckler-White, R. L. Dewar, C. E. Buckler, H. C. Lane, K. Kamada, A. Adachi, and M. A. Martin. 2007. Human immunodeficiency virus type 1 derivative with 7% simian immunodeficiency virus genetic content is able to establish infections in pig-tailed macaques. *J. Virol.* 81: 11549–11552.
8. Goulder, P. J., and D. I. Watkins. 2004. HIV and SIV CTL escape: implications for vaccine design. *Nat. Rev. Immunol.* 4: 630–640.